CR 73067

Alpha Research, Inc.
Report No. 66-3426-1
15 December 1966

AERODYNAMIC STUDIES OF NON-PLANAR AND NEAR-CIRCULAR MOTIONS

by
James E. Brunk

Summary Report for
Contract NAS 2-3426

Prepared for

NASA Ames Research Center
Moffett Field, California

Copy____ of____

TABLE OF CONTENTS

FOREWORD

This report was prepared under NASA contract NAS 2-3426, by Alpha Research, Inc. The contract was monitored by Mr. Murray Tobak, NASA Ames Research Center.

The principal investigator for this contract was Mr. James E. Brunk. Consulting services were provided by Mr. Ray Rodman. The effort was carried out from February 1966 through December 1966.

The author is grateful to both Mr. Murray Tobak and Mr. T. Coakley of the Ames Research Center for their helpful suggestions.

SUMMARY

The polar form of the equations of yawing motion for a symmetric missile are used to investigate the general nature of circular limit-cycles and non-planar motion. The polar equations are derived both directly from Euler angle variables and by transformation from the complex-variable aeroballistic equations. The difference between the two developments are noted. An aerodynamic expansion for the polar equations is developed by transformation of the Maple-Synge terms. The physical significance of the new aerodynamic terms is discussed and the concepts of circular motion damping and dynamic Magnus effect are described.

Using the exact equations of yawing motion, it is shown that circular limit cycles exist even when the aerodynamic coefficients are linear in angle of attack, as long as the Magnus moment is present. The stability of near-circular motions is shown to be readily determined by the use of pertubation equations derived from the polar equations of motion. This approach permits both geometric and aerodynamic non-linearities to be considered simultaneously without difficulty. The resulting stability criteria for a non-spinning missile with cubic aerodynamic coefficients are shown to be identical to results obtained by C. Murphy using quasi-linear theory.

Supplementing the analytical work is a review of the aerodynamic flow phenomena which affect non-planar motion by generation of forces and moments in the Magnus plane. Suggestions are made for additional experimental work to obtain the effect of angle of attack plane rotation.

I. INTRODUCTION

This report describes exploratory analytical investigations of non-planar and near-circular motions of symmetric missiles, both with and without axial spin. For the most part, these investigations are made using the equations for pitch-yaw motion in polar form.

Non-planar and circular-type motions* are exhibited, not infrequently, in full-scale vehicles such as sounding rockets, re-entry bodies, and a wide variety of tactical and air-to-surface weapons. In most instances these motions are due to the effect of the launch conditions, gyroscopic precession, or slight asymmetries combined with roll, and are well damped except possibly at pitch-roll resonance. However, in some instances there is observed a tendency for sustained circular motion which grows, in some cases, to very large amplitude. These later motions, which are of considerable concern, are to a great extent associated with the presence of Magnus-type moments or some type of non-linear damping.

While the basic linear aeroballistic theory** accounts very well for the non-planar motions resulting from initial conditions, gyroscopic effects, and the combined effects of asymmetry and roll, its use for studying motions due to Magnus-type moments is severely limited and, of course, non-linear damping moments are not within the scope of a linear theory. It is also rather well

---

* Circular motions are a particular non-planar motion wherein the angle of attack approaches or is held to a constant value. Our interest in this report is with motions which are predominantly non-planar.

** The basic linear aeroballistic theory, as developed by Murphy, Nicolaides, and others, makes use of non-rolling coordinates and exploits aerodynamic symmetry through introduction of complex variables for the angle of attack and cross angular velocity.

known that the linear theory does not predict a sustained circular motion for a symmetric missile. Although much effort has gone into extending the aeroballistic theory to account for aerodynamic nonlinearities,* there are three areas which have not received sufficient attention, namely:

1. The effect of geometric nonlinearities.
2. The description of the aerodynamic nonlinearities associated with rotation of the angle of attack plane or aerodynamic asymmetry with respect to the angle of attack plane.
3. The application of the nonlinear theory to determination of aerodynamic coefficients and derivatives from experimental data, particularly that obtained from wind tunnel tests.

The latter is essential if experimental data are to be used for predicting the flight behavior of arbitrary configurations. In the present treatment, which involves a new formulation of the equations of motion, a concerted effort is made to bring the above factors into clearer focus.

The impetus for the present work was a study of spinning bodies at very large angle of attack.[1] These early investigations were concerned with the attitude and stability of cylinder-like bodies in flat spins or very large angle of attack coning motions. To treat this problem, a pertubation technique was adopted similar to that used by Klinar & Grantham[2] for studying aircraft spins. However, new equations of motion were required which would not only accommodate large axial roll rates, but also a very wide range of angle of attack. As a result, it was found that the flat spin problem could be simulated quite well with two exact nonlinear moment equations, the first describing the motion in the angle of attack plane, and the second describing the rotational motion of the angle of attack plane itself. With such a formulation, the aerodynamic

* The work of Charles H. Murphy of BRL is particularly noteworthy.

coefficients for pitch and yaw could be independent, in contradiction to the assumptions of aerodynamic symmetry assumed at small angles of attack. It was particularly noteworthy that approximation of the aerodynamic damping at angles of attack at or approximating ninety degrees, showed that two different values existed, one value applicable to rotation of the body in the angle of attack plane, a second value applicable to the rotation of the body in a plane normal to the angle of attack plane.

A most noteworthy aspect of the new formulation was that steady-state constant-angle-of-attack solutions were obtained for practically all types of Magnus moments. As a result, we have referred to this approach as a "circular-motion theory." When the generality of the circular motion theory was fully realized, it became apparent that the same approach (and even the same equations) were applicable at small angles of attack, the domain of the aeroballistic theory.

A comparison of the equations, however, immediately presented a dilema, since, in the circular motion theory separate aerodynamic variables exist for the angle of attack and Magnus planes,* whereas in the aeroballistic theory single coefficients are used to describe both components of the complex pitch-yaw motion. This raised a question as to the appropriate aerodynamic system, even at small angles of attack. So far, this question has been resolved only for angles of attack approaching zero, where it has been shown that the angular velocity damping derivatives are identical for the angle of attack and Magnus planes. For larger angles of attack, it appears that nonlinear damping terms will have to be included in the aeroballistic theory.

---

* Throughout this report, the Magnus plane refers to a plane normal to the angle of attack plane. The Magnus plane also contains the missile axis of symmetry.

A second concern growing from comparison of the aeroballistic and circular motion equations was that the former did not readily reveal the existence of circular limit cycles for a wide variety of conditions, not even for a linear Magnus moment. These differences could be traced, in part, to the linearization of the inertial terms in the aeroballistic equations of motion. Thus it appeared, that for investigation of circular motion, the inertial terms in the equations of motion must be retained in their exact nonlinear form.

Another area of uncertainty was the non-rolling coordinates used in the aeroballistic equations, as these do not describe the angle of attack plane rotation precisely. Thus it was felt that a clearer separation of the effects of spin and angle of attack plane rotation should be possible with the circular motion theory.

The aerodynamic subtleties of non-planar motion appear in the aeroballistic theory as complex nonlinear aerodynamic coefficients. The nature of these coefficients has been explained by C. Murphy in several papers, but yet the complex-variable formulation has not encouraged a concerted effort to determine the coefficients experimentally. This fault is corrected in the present effort, by adoption of a new set of aerodynamic coefficients, which are related to readily observable and measurable motion parameters.

With the new formulation such phenomena as "circular motion damping" and "dynamic Magnus effect" take on a meaningful significance.

The scope of the present study is quite vast, but because of the limitations of program funding, much of the work has had to be of an exploratory nature. The main objectives of the present effort have been as follows:

1. To compare the aeroballistic and circular motion theories.
2. To arrive at an improved aerodynamic formulation for non-planar motions.

3. To predict the motion and stability of axisymmetric bodies under the influence of various Magnus phenomenon.

4. To show the adaptability of the small pertubation theory and the polar-form of the equations of motion to the analysis of near-circular motions.

5. To review, investigate and extend the available methods of predicting the aerodynamic force distribution on bodies of revolution at large angles and in non-planar motion, and the subsequent determination of stability coefficients.

6. To review and suggest improved methods for experimental determination of aerodynamic coefficients associated with non-planar and circular motion.

II. APPLICATION OF EXISTING MOTION THEORY TO THE CIRCULAR MOTION PROBLEM

The equations of yawing motion in polar form have the advantage that the total angle of attack is represented by a single rotating vector. In turn, the motion represented by this single vector can be expressed by two equations in real variables. For near-circular motions, the polar equations not only provide a better physical picture of the dynamics, but also permit considerable mathematical simplification. In the case of circular limit cycles, the amplitude and frequency are in most cases obtainable directly from algebraic equations, since all of the derivatives approach zero except that which represents the rotation of the angle of attack vector.

In this section of the report we will review the form of the polar equations both as they are developed by transformation from complex variable equations, and as derived directly from Euler angles. Each approach has received previous attention by aerodynamicists and mathematicians. Our present interest is in the way of introduction, and we will take up the more general development of the polar equations in Section III. In addition, we will briefly consider, here, the nature of the circular limit cycles indicated by the two different developments of the polar equations.

A. Development of Polar Equation of Motion by Transformation from Complex Variables

One method of obtaining a set of polar equations is by suitable transformation of the aeroballistic equations, * which are usually of the form

$$\tilde{\xi}'' + C_1 \tilde{\xi}' + C_2 \tilde{\xi} = C_3 \qquad 1)$$

* The simplicity of Equation 1) is often exploited for investigation of time varying coefficients and specific aerodynamic nonlinearities.

where $\tilde{\xi}$ is the complex yaw and the C's are complex quantities which may be constants or highly nonlinear functions. The complex yaw is usually with respect to non-rolling coordinates and the necessary transformation to the polar form is

$$\tilde{\xi} = \delta e^{i\theta} = \beta + i\alpha \qquad 2)$$

where the variables are described in sketch below:

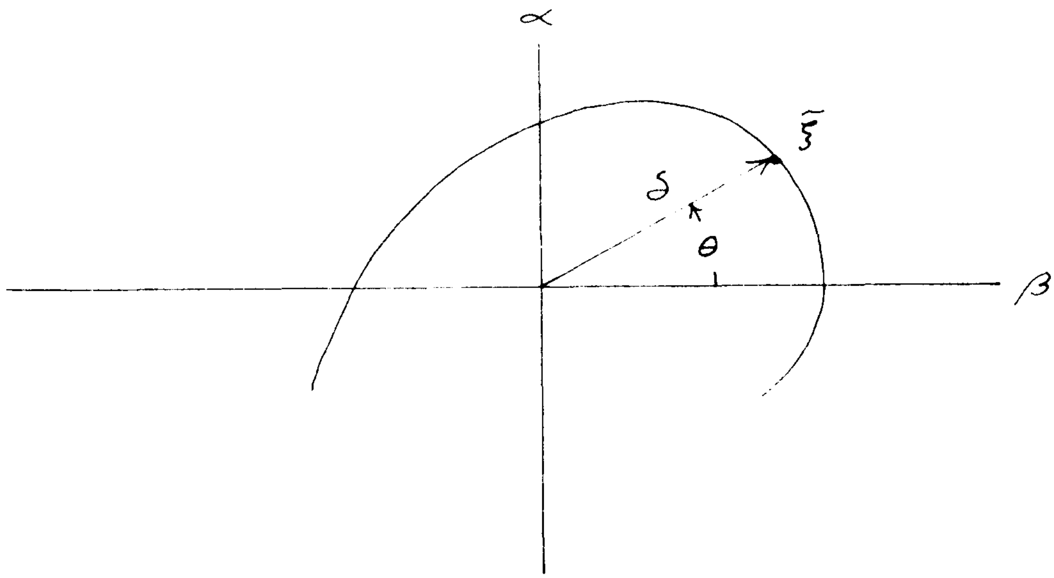

After performing the transformation, the real and imaginary terms can be separated into two separate scalar equations. From the linear form of equation 1), as derived by C. Murphy, reference 3, we obtain in Murphy's notation

$$\delta'' - \delta(\theta')^2 + H\delta' + P\delta\theta' - M\delta = 0 \qquad 3)$$

$$2\delta'\theta' + \theta''\delta + H\delta\theta' - P\delta' - PT\delta = 0 \qquad 4)$$

Obviously, more complicated polar equations result when nonlinear terms are included in 1), However, it must constantly be kept in mind that all of the assumptions involved in equations 1) will be retained in 3) and 4). This point will be discussed in more detail later in the paper.

Zaroodny, ref. 4, has further transformed 3) and 4) from circular to spiral yaw by use of the transformation

$$\delta = \delta_o e^{\int_0^s \tau \, ds} \quad ; \quad \delta' = \tau \delta$$

where τ represents the spiral motion and s is the independent variable. Zaroodny goes on to examine the effect of nonlinear Magnus moment on the spiral yaw by an iteration technique.

Haseltine, ref. 5, has examined the nonlinear form of 3) and 4), which includes the geometric nonlinearity in the angle of attack, i. e., the inclusion of terms in γ, where $\gamma = \cos \tilde{\alpha}$. Haseltine, through a rigorous as well as general analysis has shown that certain periodic solutions can be determined by pertubation theory. The work of Haseltine is particularly noteworthy, in that it shows that the pertubation equations derived from equations 3) and 4) will lead to the same conclusions regarding periodic solutions and the stability as do the methods employed by Murphy, ref. 6. This fact will be clearly shown in a subsequent section of the report.

The inherent shortcoming of the transformed equations is that equation 1) usually contains approximations for the geometric nonlinearities. When equation 1) is derived in its most general form (see, for example, Appendix A of ref. 7) there exists two parameters in the C's: ω the axial spin rate, and Ω_1, the rotation of the y z moving coordinates. However, in the application of equation 1), Ω_1 is usually deleted by the selection of non-rolling coordinates. Thus, with $\Omega_1 = 0$, there is the added complication of the motion generated by the moving axes themselves. This very important question has received some attention by Murphy from the standpoint of reduction of ballistic range data.[7] More light will be shed on this problem as a result of the present analyses.

B. Development of Polar Equations from Euler Angle Variables

The direct formulation of the polar equations for the three angular degrees of freedom follows from selection of Euler angles which represent the orientation of the missile axis of symmetry with respect to an appropriate inertial reference. In general it will be convenient to make the inertial reference coincident with the total velocity vector. This precludes the effects of translation, nevertheless the equations are useful for studying motions such as those of wind tunnel models, and have the advantage that the inertial moment terms are exact. An axis system often employed is illustrated below:

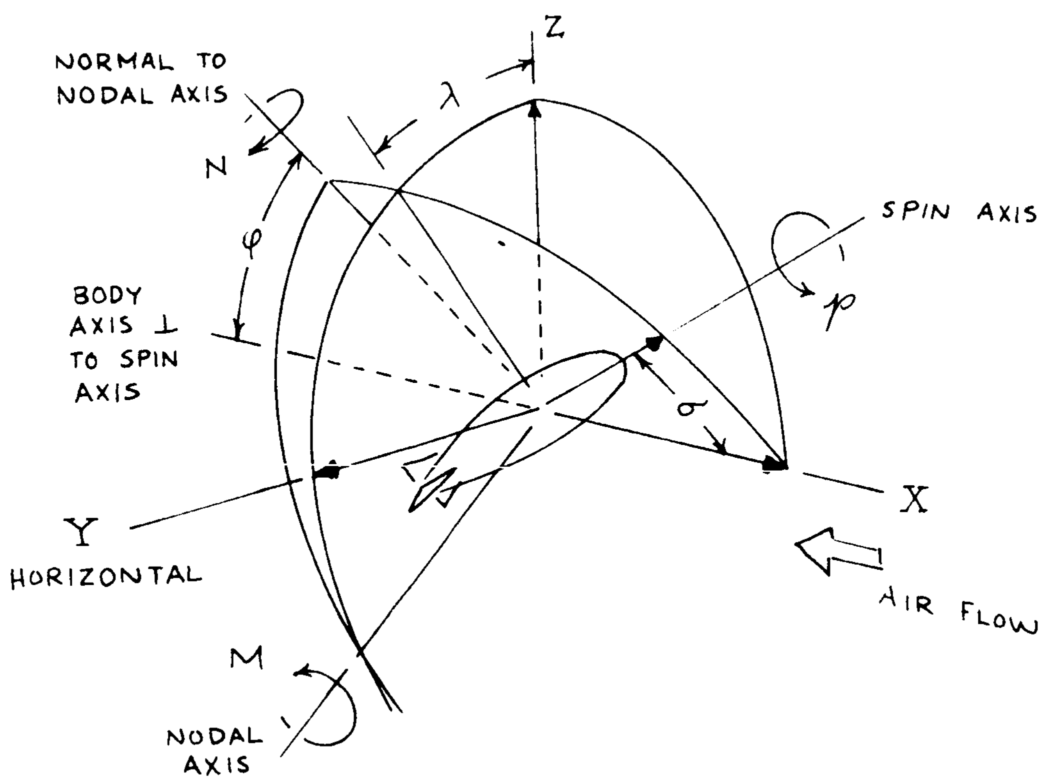

The equations of motion can be shown to be

$$L = I_x \dot{p} \qquad 5)$$

$$M = I\ddot{\sigma} - I\dot{\lambda}^2 \sin\sigma \cos\sigma + I_x p \dot{\lambda} \sin\sigma \qquad 6)$$

$$N = I\ddot{\lambda} \sin\sigma + 2I\dot{\lambda}\dot{\sigma} \cos\sigma - I_x p \dot{\sigma} \qquad 7)$$

In contrast to equations 3) and 4), the above equations are basically nonlinear.

These equations are effectively those of a top with appropriate aerodynamic terms added. This form of the polar equation was used by Bird and Lichtenstein, ref. 30, for studying the motion of a wind tunnel model with three degrees of angular freedom. Apparently Bird and Lichtenstein did not recognize the fact that steady-state or pertubation solutions could be obtained analytically from 6) and 7), and their investigations were restricted to solutions obtained by computer.

The distinguishing feature about equations 5), 6) and 7) is that they define the location of the angle of attack plane precisely with respect to inertial space. In contrast, the orientation of the angle of attack plane is not known precisely with aeroballistic non-rolling axes when the angle of attack is finite and the motion non-planar.

The inertial terms in equations 6) and 7) are similar to those in the transformed linear equations 3) and 4), except that the former equations involve trigonometric functions of σ , the angle of attack

C. Circular Motion Solutions

A circular motion solution can be obtained from the polar equations 3) and 4) whenever we can establish finite values of δ and θ' for $\delta'' = \delta' = \theta' = 0$. However, it is at once obvious that the linear equations

3) and 4) lead only to the trivial solution $\delta = 0$. From 3) we obtain the usual precessional and nutational frequencies,

$$\theta' = \frac{P}{2} \pm \frac{1}{2}\sqrt{P^2 - 4M} \tag{8}$$

while from 4) we obtain the additional relationship

$$\theta' = \frac{PT}{H} \tag{9}$$

To obtain a finite value of δ nonlinear terms must be added to equations 3) and 4) such that δ does not factor out of either 3) and 4). An interesting consequence of this is the case of zero spin with nonlinear damping, H a function only of δ^2. For steady circular motion this new H term will drop out of 3), because $\delta \rightarrow 0$, and will appear only in equation 4). But a solution to 4) will be obtained only if $\theta' = 0$. Therefore, nonlinear damping proportional to δ^2 cannot lead to circular motion. This result has also been obtained by a nonlinear analysis of equation 1). It should also be noted at this point that a linear Magnus moment does not lead to a circular motion solution from equations 3) and 4).

Now let us examine the possibility of circular motion solutions from equations 6) and 7). Again, letting the motion approach steady-state we can set $\ddot{\sigma} = \dot{\sigma} = \ddot{\lambda} = 0$ and obtain

$$M = -I\dot{\lambda}^2 \sin\sigma \cos\sigma + I_x p \dot{\lambda} \sin\sigma \tag{10}$$

$$N = 0 \tag{11}$$

Equation 11) merely states that the total aerodynamic yawing moment must equal zero. *

---

* From examination of the coordinates in the sketch on page 9, it can be seen that N moment corresponds to the Magnus plane while the M moment corresponds to the angle of attack plane.

Consider first the case where the aerodynamic moments are linear in σ. Equation 11) can now be written as

$$C_{n_{p\sigma}} \hat{p}' \sigma + C_{n_{\sigma\dot{\lambda}}} \sigma \lambda' = 0$$

In addition to the trivial solution $\sigma = 0$, we obtain

$$\lambda' = -\frac{C_{n_{p\sigma}} \hat{p}}{C_{n_{\sigma\dot{\lambda}}}}$$

which when substituted into

$$\frac{C_{m_\sigma} \sigma}{I'} = -\lambda'^2 \sin\sigma \cos\sigma + \frac{I_x}{I} \lambda' \hat{p} \sin\sigma$$

leads to

$$\cos\sigma = \frac{-\dfrac{C_{m_\sigma} \sigma}{I' \sin\sigma} - \left(\hat{p}\dfrac{I_x}{I}\right)\left(-\dfrac{C_{n_{p\sigma}} \hat{p}}{C_{n_{\sigma\dot{\lambda}}}}\right)}{\left(\dfrac{C_{n_{p\sigma}} \hat{p}}{C_{n_{\sigma\dot{\lambda}}}}\right)^2} \tag{12}$$

Solutions to equation 12) will exist for a wide range of σ, provided $C_{n_{p_\sigma}}$ is sufficiently large. Thus, a family of steady-state circular motion solutions are obtained from equations 6) and 7), even with linear aerodynamics!

The reason for this can easily be traced to the fact that $\cos\sigma$ appears in equation 10), thus not permitting σ to factor out of that equation.* If the usual small angle approximation, $\cos\sigma = 1$, were introduced prior to formulation of equation 10), the same difficulty would be experienced in obtaining a steady-state solution as was the case with equations 3) and 4).

For illustrative purposes, equation 12) is plotted in Figure 1) for some representative values of the aerodynamic and inertial parameters.

---

* This is true particularly when M is a linear function of $\sin\sigma$, which is the case when the angle of attack is defined to be $\frac{v + iw}{V}$.

The solutions are shown as $\hat{p}$ versus σ, where $\hat{p}$ = pd/V is now a parameter. For $C_{m_\sigma} < 0$, the solution curves are in the range $0 < \sigma < \pi/2$, while for $C_{m_\sigma} > 0$ the solution curves are in the range $\frac{\pi}{2} < \sigma < \pi$. It will be noted that for small values of the Magnus moment coefficient, solutions are not always obtained. However, when both the Magnus moment coefficient and the spin rate parameter, $\hat{p}$, are large, circular motion solutions are always obtained.

To obtain a complete steady-state solution of all three moment equations, it is only necessary to superimpose on Figure 1 the actual values of the spin rate parameter as a function of σ. As can be seen from the shape of the curves, the magnitude and variation of the actual spin rate with σ will have a significant effect on the amplitude of the circular motion. Particularly, if the spin rate varies only slightly with σ, the circular motion solutions will tend to correspond to values of σ closer to 90 degrees than to either zero or 180 degrees. It is of interest in these latter cases that for very large spin, a positive Magnus moment leads to circular motion solutions with $\sigma < \pi/2$, regardless of the size of C_{m_σ}. Likewise for negative Magnus moment and very large spin, $\sigma > \pi/2$.

With slight modification of the usual linear aerodynamic system it is possible to obtain other circular motion solutions. For example, Tobak and Lessing[27] have obtained circular motion solutions by re-defining the Magnus and damping coefficients.

By replacing the classical Magnus moment with a side moment*, which has a linear dependency upon angle of attack, some additional and

* The linear side-moment is not consistent with aerodynamic symmetry considerations. Yet, moments closely approximating a linear side moment have been measured on finned rockets where the fin planes were not aligned with the angle of attack plane.

very interesting results are obtained. In this case we consider only a lunar circular motion.

$$p = \dot{\lambda} \cos \sigma \qquad 13)$$

For this case the steady-state solutions are obtained from

$$N_\sigma \sigma + N_{\sigma\dot{\lambda}} \sigma \dot{\lambda} = 0$$

$$-M_\sigma \sigma = \dot{\lambda}^2 \sin \sigma \cos \sigma \left[1 - \frac{I_x}{I} \right]$$

with the result that

$$\frac{\sin \sigma \cos \sigma}{\sigma} = \frac{-M_\sigma / I}{\left(1 - \frac{I_x}{I}\right)\left(- \frac{N_\sigma}{N_{\sigma\dot{\lambda}}}\right)^2} \qquad 14)$$

Here again, circular solutions will be obtained if N_σ is sufficiently large. It will be observed that p and $\dot{\lambda}$ must have the same sign for $\sigma < \frac{\pi}{2}$. Thus for $p > 0$ and $N_{\sigma\dot{\lambda}} < 0$, we must have a positive side moment, $N_\sigma > 0$.

The above exercises, (based on elementary equations) are presented for the express purpose of illustrating the contribution of geometric non-linearities to limit circular motion. Also, we have shown the significance of the N moments, which can result in a frequency, $\dot{\lambda}$, independent of the pitch natural frequency, and thus permit a simultaneous solution for σ and $\dot{\lambda}$.

One further remark can be made about equations 12) and 14): It will be noted that the numerator of the right hand side of each equation depends upon the air density, through the aerodynamic parameter M_σ, while the denominator of each equation is independent of air density and depends only upon the constant frequency, $\dot{\lambda}$. It is therefore possible to obtain solutions to 12) and 14) at high altitudes, even though no solution may exist at low altitudes. Therefore, even small Magnus-type moments can be expected to produce coning motions of sounding rocket vehicles at very high altitudes.

D. Effect of Aerodynamic Rotational Symmetry

A distinguishing mark between the polar equations obtained by transformation (equations 3 and 4) and those obtained directly from the Euler angles (equations 6 and 7) is that, in the former, aerodynamic rotational symmetry is implied, while in the latter, one is free to select separate aerodynamic characteristics for the angle of attack and Magnus planes. This fact is made very evident by closer inspection of equations 3) and 4). It will be noted that the damping parameter, H, is forced to appear in both equations 3) and 4) while the overturning moment parameter, M, appears only in 3) and the Magnus moment parameter, T, appears only in 4). For steady circular motion only, the H and T terms remain in 4), so that either H or T will affect the frequency, θ', as obtained from equation 9). The significance of the above remarks is as follows: for systems which exploit aerodynamic rotational symmetry, there is a forced inter-relationship between the Magnus moment and the damping moment. This fact makes the use of linear equations 3) and 4) very suspect for the analysis of experimental motions, where the exact form of either H or T may not be precisely known. A most obvious consequence of this would be that of a slight nonlinearity in the Magnus moment being interpreted as a nonlinear damping moment.

III. A NEW FORMULATION OF THE POLAR EQUATIONS

In the preceding section some of the advantages and disadvantages of the two different types of polar equations were made apparent. These factors have led to the derivation of a new set of equations, which are an extension of the moment equations with the Euler angles as dependent variables. These new equations incorporate the effect of lateral translation, which is known to have an important effect on aerodynamic damping. Finally, we will show the difference between the new formulation and the exact fourth order complex variable equations.

Equations of Motion, Rotational Degrees of Freedom

For the purpose of comparing with the aeroballistic theory as well as following the original large angle of attack motion theory of ref. 1, the Euler angle notation noted below is utilized.

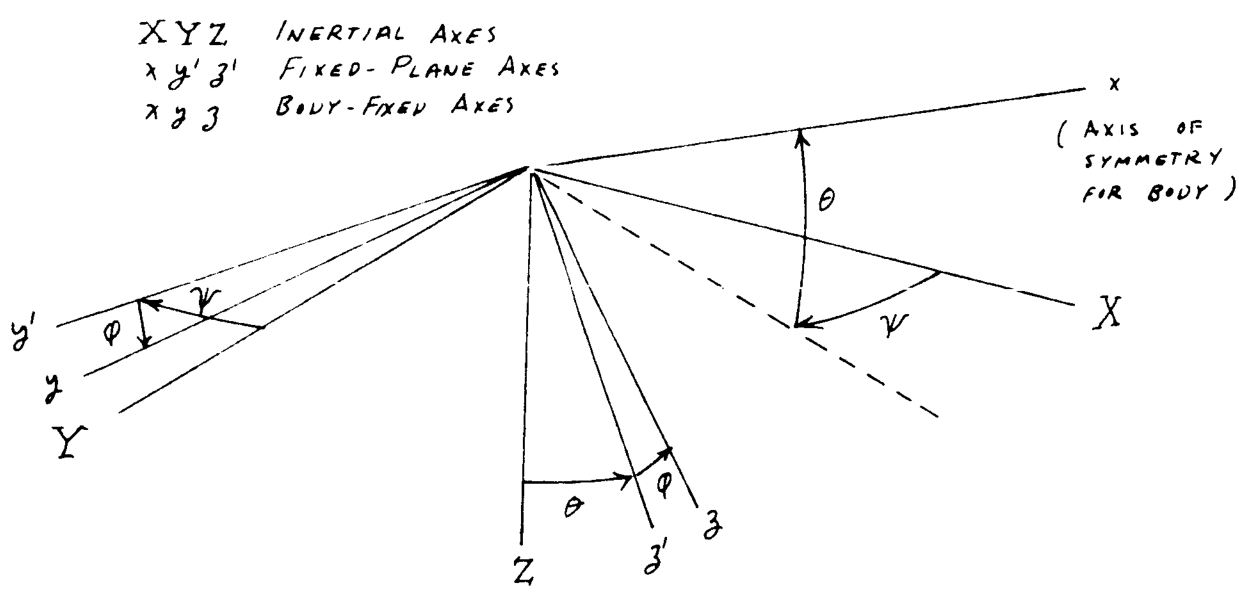

If x y' z' are fixed-plane axes, i.e., y' always is the XY plane, the angular velocities of the body and the triad can be expressed as

$$\Omega_x = -\dot{\psi}\sin\theta \qquad \omega_x = p = \dot{\phi} - \dot{\psi}\sin\theta$$
$$\Omega_{y'} = \dot{\theta} \qquad \omega_{y'} = q = \dot{\theta}$$
$$\Omega_{z'} = \dot{\psi}\cos\theta \qquad \omega_{z'} = r = \dot{\psi}\cos\theta$$

where $\dot{\phi}$ represents the roll of the missile with respect to x y' z' coordinates. These can be substituted into the fundamental equation of motion for moving axes systems,

$$\vec{M} = [I]\dot{\vec{\omega}} + \vec{\Omega} \times [I]\vec{\omega} \qquad 15)$$

to obtain the moment equations. In the work which follows we assume axial mass symmetry, and also x to be a principal axis such that

$$[I] = \begin{bmatrix} I_x & & \\ & I & \\ & & I \end{bmatrix}$$

The resulting scalar moment equations are

$$L = I_x \dot{p} \qquad 16)$$

$$M = I\ddot{\theta} + I_x p r + I r^2 \tan\theta \qquad 17)$$

$$N = I\dot{r} - I_x p\dot{\theta} - I r\dot{\theta}\tan\theta \qquad 18)$$

or equivalently

$$L = I_x \dot{p}$$
$$M = I\ddot{\theta} + I_x p\dot{\psi}\cos\theta + I\dot{\psi}^2\cos\theta\sin\theta$$
$$N = I\ddot{\psi}\cos\theta - I_x p\dot{\theta} - 2I\dot{\psi}\dot{\theta}\sin\theta$$

A simple transformation from equations 16) - 18) to equations 5) - 7) is possible by use of the relationships

$$\lambda = \psi$$

$$\sigma = \pi/2 + \theta$$

We now consider the effect of translational motion. The fixed-plane force equations can be derived in a manner similar to the moment equations with the following results:

$$\left.\begin{aligned} F_x &= m\left(\dot{u} + w\dot{\theta} - v\dot{\psi}\cos\theta\right) \\ F_{y'} &= m\left(\dot{v} + w\dot{\psi}\sin\theta + u\dot{\psi}\cos\theta\right) \\ F_{z'} &= m\left(\dot{w} - v\dot{\psi}\sin\theta - u\dot{\theta}\right) \end{aligned}\right\} \qquad 19)$$

To couple these equations with the moment equations it is convenient to select new variables to represent the translational motion. In accordance with the following sketch we select ϵ to represent the deflection of the velocity vector in the x y' plane, and $\Delta\dot{\psi}$ to represent any additional rotation of the fixed-plane axes required to make the total velocity lie in the x Z plane

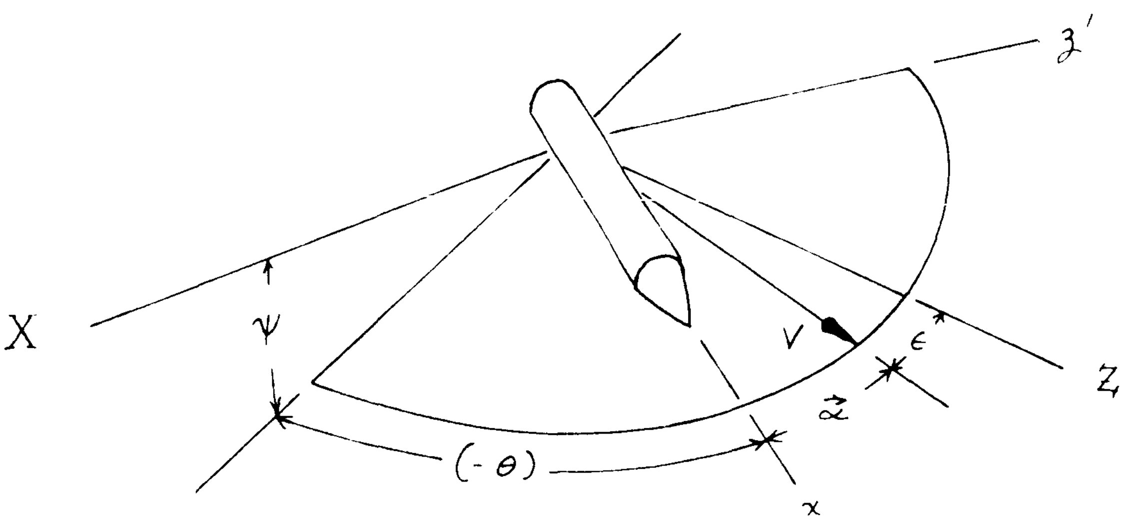

We now introduce the relationships

$$\epsilon = \pi/2 - (-\theta) - \vec{\alpha} \qquad 20)$$

$\dot{\psi} + \Delta\dot{\psi}$ = rotation of angle of attack plane

Since our interest is basically in the yawing motion, we can restrict our attention to values of ϵ and $\Delta\dot{\psi}$ which approach zero, retaining, however, the effects of the derivatives of ϵ and $\Delta\dot{\psi}$. We also assume here that the lift force is the predominant force affecting the lateral translation. These assumptions allow us to neglect the $v\dot{\psi} \sin\theta$ term in equation 19c) and to set $F_y' = 0$ in equation 19b). With the aid of the relationships

$$\begin{aligned}
\dot{\theta} &= \dot{\vec{\alpha}} + \dot{\epsilon} \\
w &= V \sin \vec{\alpha} \\
u &= V \cos \vec{\alpha} \\
(\ )' &= \frac{d}{V}(\ )^{\cdot} \\
\frac{V'}{V} &= -\frac{\rho s d}{2m} C_D \\
F_z' &= C_N \frac{\rho s d}{2m}
\end{aligned} \qquad 21)$$

it can be shown that

$$\epsilon' = \frac{\rho s d}{2m} C_L = \frac{\rho s d}{2m} C_{L_\alpha} \vec{\alpha} \qquad * \qquad 22)$$

and

$$\epsilon'' = \frac{\rho s d}{2m} C_{L_\alpha} \vec{\alpha}' + \frac{\rho s d}{2m} \vec{\alpha}\left(C_{L_\alpha}\right)' \qquad 23)$$

From 19b) we obtain, by expanding $\sin(\vec{\alpha} + \epsilon)$ and $\cos(\vec{\alpha} + \epsilon)$

$$\dot{v} = -V(\dot{\psi} + \Delta\dot{\psi})\epsilon + \frac{V(\dot{\psi} + \Delta\dot{\psi})\epsilon^3}{6} + \cdots \qquad 24)$$

To the first order in ϵ, this is exactly the acceleration cross product $V\epsilon \times \dot{\psi}$, which is obtained directly for $\dot{v} = 0$, with our rotating coordinates.

---

* The singular dependence of C_L on $\vec{\alpha}$ is not implied, but is assumed for convenience. Comparison with aeroballistic theory will show that the dependence of C_L on $\vec{\alpha}'$ must also be considered, if comparison is to be made with aeroballistic equations containing $C_{N_{\alpha'}}$ terms.

The value of $\Delta\dot{\psi}$ desired, is that which will make $\dot{\phi} = -\nu\dot{\psi}\epsilon$. Thus from equation 24)

$$\Delta\dot{\psi} = \frac{\dot{\psi}\epsilon^2}{\nu} + \text{higher order terms.}$$

It is now seen that to the first order of ϵ, it is possible to neglect $\Delta\dot{\psi}$.

Equations 17) and 18) can now be written in the following form. *

$$\begin{aligned}(\vec{\alpha}'' + \epsilon'') + (\vec{\alpha}' + \epsilon')\left(-\frac{\rho S d}{2m} C_D\right) + \frac{pd}{V}\frac{I_x}{I}\psi' \sin(\vec{\alpha}+\epsilon) \\ - (\psi')^2 \sin(\vec{\alpha}+\epsilon)\cos(\vec{\alpha}+\epsilon) = \frac{\rho S d^3}{2I}\left[C_{M_\alpha}\vec{\alpha} + C_{M_{\dot{\theta}}}(\vec{\alpha}'+\epsilon') + C_{M_{\dot{\alpha}}}\vec{\alpha}'\right]\end{aligned} \tag{25}$$

$$\begin{aligned}\left[\psi'' + \psi'\left(-\frac{\rho S d}{2m}C_D\right)\right]\sin(\vec{\alpha}+\epsilon) - \frac{I_x}{I}\frac{pd}{V}(\vec{\alpha}'+\epsilon') + 2\psi'\theta'\cos(\vec{\alpha}+\epsilon) \\ = \frac{\rho S d^3}{2I}\left[C_{n_r}\psi'\sin(\vec{\alpha}+\epsilon) + C_{M_{p\alpha}}\frac{pd}{V}\vec{\alpha}\right]\end{aligned} \tag{26}$$

Substitutions of 22) and 23) into 25) and 26) gives the final form of the polar equation with linear aerodynamics.

$$\begin{aligned}\vec{\alpha}'' + \left[\frac{\rho S d}{2m}C_{L_\alpha} - \frac{\rho S d}{2m}C_D - \frac{\rho S d^3}{2I}\left(C_{M_{\dot{\theta}}} + C_{M_{\dot{\alpha}}}\right)\right]\vec{\alpha}' \\ + \frac{pd}{V}\frac{I_x}{I}\psi'\sin(\vec{\alpha}+\epsilon) - (\psi')^2\sin(\vec{\alpha}+\epsilon)\cos(\vec{\alpha}+\epsilon) \\ - \left[\frac{\rho S d^3}{2I}C_{M_\alpha} - \frac{\rho S d}{2m}C_{L_\alpha}'\right]\vec{\alpha} = 0\end{aligned} \tag{27}$$

$$\begin{aligned}\psi''\sin(\vec{\alpha}+\epsilon) - \frac{I_x}{I}\frac{pd}{V}\vec{\alpha}' + 2\psi'\vec{\alpha}'\cos(\vec{\alpha}+\epsilon) \\ + \psi'\left[2\frac{\rho S d}{2m}C_{L_\alpha}\cos(\vec{\alpha}+\epsilon)\vec{\alpha} - \frac{\rho S d}{2m}C_D\sin(\vec{\alpha}+\epsilon) - \frac{\rho S d^3}{2I}C_{n_r}\sin(\vec{\alpha}+\epsilon)\right] \\ + \left(\frac{pd}{V}\right)(\vec{\alpha})\left[-\frac{\rho S d^3}{2I}C_{M_{p\alpha}} - \frac{\rho S d}{2m}\frac{I_x}{I}C_{L_\alpha}\right] = 0\end{aligned} \tag{28}$$

* The aerodynamic coefficients used here correspond to those appearing in the aeroballistic equations 3) and 4).

It is now worthwhile to carefully examine the differences between 27) and 28) and the aeroballistic equations. The most exact form of equation 1) is, for the same assumptions as above, *

$$\left[1 + J_{NA}\right]\xi'' + \left[H - \frac{\gamma'}{\gamma} - i\left(P - 2\hat{v} - J_{NA}\hat{v}\right)\right]\xi' + \left[-M + \hat{v}(P - \hat{v}) - i\left(PT - \hat{v}\left(H - \frac{\gamma'}{\gamma}\right) - \hat{v}'(1 + J_{NA})\right)\right]\xi = 0 \qquad 29)$$

where

$$\xi = \frac{u_2 + i\,u_3}{u}$$

$$\hat{v} = \frac{\Omega_1 d}{u}$$

$$u = |\vec{u}|$$

$\vec{u} = (u_1\,,\ u_2\,,\ u_3)$, velocity vector

With this formulation the rotation of the moving coordinates is specified only by Ω_1 , and hence equation 29) is valid for both non-rolling and fixed-plane axes systems.

It should be emphasized, here, that equation 29) results from combining a first order complex equation for ξ' with a first order complex equation for the cross angular velocity. Note, also, that the complex variables are describing the motion relative to the body axis of symmetry, whereas the variables in equations 25) and 26) are related to either the velocity vector or the inertial reference axes.

Now let us examine the basic differences between equations 26) and 28) and equation 29). This is most easily accomplished by transforming equation

---

* This equation is derived in Appendix A of BRL Report No. 974, ref. 7. The J_{NA} terms, which are proportional to $C_{N_{\dot{\alpha}}}$, are usually omitted, but must be retained here if $C_{L_{\ddot{\alpha}}}$ is to be included in the expansion of eq. 23).

29) into polar form and taking into account the relationships between variables. We will first consider equation 29) with J_{NA} deleted. Again letting

$$\xi = \delta e^{i\theta}$$

we obtain from equation 28) after separating real and imaginary parts

$$\delta'' - \delta'(\theta' + \hat{v})^2 + \left[\frac{\rho s d}{2m}\gamma C_{L_\alpha} - \frac{\rho s d}{2m}C_D - \frac{\rho s d^3}{2I}\left(C_{M_q} + C_{M_{\dot\alpha}}\gamma\right)\right]\delta' - \frac{\gamma'}{\gamma}\delta' + \frac{pd}{V}\frac{I_x}{I}\delta(\theta' + \hat{v}) - \gamma\frac{\rho s d^3}{2I}C_{M_\alpha} - \gamma\frac{\rho s d}{2m}\left(C_{L_\alpha}'\right) = 0 \quad 30)$$

$$2\delta'(\theta' + \hat{v}) + \delta(\theta' + \hat{v})' + \left[\frac{\rho s d}{2m}\gamma C_{L_\alpha} - \frac{\rho s d}{2m}C_D - \frac{\rho s d^3}{2I}\left(C_{M_q} + \gamma C_{M_{\dot\alpha}}\right)\right]\delta(\theta' \hat{v}) - \frac{\gamma'}{\gamma}\delta(\theta' + \hat{v}) - \frac{pd}{V}\frac{I_x}{I}\delta' - \frac{pd}{V}\frac{I_x}{I}\left[\frac{\rho s d}{2m}\gamma C_{L_\alpha} + \frac{\rho s d^3}{2I_x}\gamma C_{M_{p\alpha}}\right]\delta = 0 \quad 31)$$

To compare 30) and 31) with 27) and 28) we need to consider the following additional relationships

$$\begin{aligned}
\delta &= \sin\vec{\alpha} \\
\delta' &= \vec{\alpha}'\cos\vec{\alpha} \\
\delta'' &= \vec{\alpha}''\cos\vec{\alpha} - (\vec{\alpha}')^2\sin\vec{\alpha} \\
\gamma &= \cos\vec{\alpha} \\
\gamma' &= -\vec{\alpha}'\sin\vec{\alpha} \\
(\theta' + \hat{v}) &\approx \psi'(\cos\vec{\alpha} - \epsilon\sin\vec{\alpha}) \\
(\theta' + \hat{v})' &\approx \psi''\cos\vec{\alpha} - \psi'\vec{\alpha}'\sin\vec{\alpha} - \psi'\epsilon\cos\alpha(\alpha' + \epsilon') \\
&\quad - \psi''\epsilon\sin\vec{\alpha} - \psi'\epsilon'\sin\vec{\alpha}
\end{aligned} \quad 32)$$

In addition the coefficient notation is different, since different variables are used. Denoting the coefficients of equations 30) and 31) by subscript M and those of equations 27) and 28) by A, we have that:

1) for coefficients of angle of attack

$$(C_{ij})_M = (C_{ij})_A \frac{\vec{\alpha}}{\sin \vec{\alpha}}$$

2) for coefficients of cross angular velocity

$$(C_{ij})_M = (C_{ij})_A$$

3) for coefficients of the derivative of the angle of attack

$$(C_{ij})_M = (C_{ij})_A \frac{1}{\cos \vec{\alpha}}$$

Finally, we obtain from 30) and 31)

$$\vec{\alpha}'' + \left[\frac{\rho s d}{2m} (C_{L_\alpha})_A \frac{\vec{\alpha}}{\tan \vec{\alpha}} - \frac{\rho s d}{2m} (C_D)_A - \frac{\rho s d^3}{2I} (C_{M_q} + C_{M_{\dot{\alpha}}})_A \right] \vec{\alpha}' - (\psi')^2 \sin \vec{\alpha} \cos \vec{\alpha} + \frac{pd}{V} \frac{I_x}{I} \psi' \sin \vec{\alpha} - \frac{\rho s d^3}{2I} (C_{M_\alpha})_A \vec{\alpha} - \frac{\rho s d}{2m} (C_{L_\alpha}')_A \vec{\alpha} = 0 \tag{33}$$

$$\psi'' \sin \vec{\alpha} - \frac{I_x}{I} \frac{pd}{V} \vec{\alpha}' + 2 \psi' \vec{\alpha}' \cos \vec{\alpha} + \left[\frac{\rho s d}{2m} (C_{L_\alpha})_A \frac{\vec{\alpha}}{\tan \vec{\alpha}} - \frac{\rho s d}{2m} (C_D)_A - \frac{\rho s d^3}{2I} (C_{M_q} + C_{M_{\dot{\alpha}}})_A \right] \psi' \sin \vec{\alpha} - \frac{pd}{V} \frac{I_x}{I} \left[\frac{\rho s d}{2m} C_{L_\alpha} + \frac{\rho s d^3}{2 I_x} C_{M_{p\alpha}} \right] \vec{\alpha} = 0 \tag{34}$$

In equations 33) and 34) terms of order $\vec{\alpha} \epsilon$, $(\vec{\alpha} \epsilon)^2$, $\vec{\alpha}' \epsilon$, $\epsilon' \epsilon$, and $\vec{\alpha}^2 \epsilon'$ are neglected.

Equations 33) and 34) are identical with 27) and 28), except for differences in the damping parameters, particularly the coefficients of $\psi' \sin(\bar{\alpha} + \epsilon)$ and $\psi \sin(\bar{\alpha})$ in equations 28) and 34), respectively. First, we see that the damping parameter in equation 28) involves only C_{n_r}, while the aeroballistic damping parameter in equation 34) is $C_{M_q} + C_{M_{\dot{\alpha}}}$. The second difference is that in equation 34) the lift contribution to the damping is $\frac{\rho S d}{2m}(C_{L_{\dot{\alpha}}})_A \psi' \frac{\bar{\alpha} \sin\bar{\alpha}}{\tan\bar{\alpha}}$ whereas in equation 28) we have $\frac{\rho S d}{m} C_{L_{\dot{\alpha}}} \psi' \bar{\alpha} \cos(\bar{\alpha} + \epsilon)$.

In contrast to the above, inclusion of $C_{L_{\dot{\alpha}}}$ in equation 22) and J_{NA} in equation 29) leads to equivalent terms in the polar equations. The principal contribution of J_{NA} to equation 34) is $2 J_{NA} \psi' \bar{\alpha}'$, while the corresponding term in 28) is $2\left(\frac{\rho S d}{2m} C_{L_{\dot{\alpha}}}\right)\left(\cos(\alpha + \epsilon)\right) \psi' \bar{\alpha}'$. Note that the factor 2.0 appears in both of these terms.

The reasons for the small difference in the $C_{L_{\dot{\alpha}}}$ damping parameters between the exact transformed aeroballistic equations and the equations derived herein, is not fully understood at this time. It remains to be shown whether this difference is due to 1) the method of including translation into the Euler angle equations, 2) the transformation relationships, 3) the combined effect of second order terms, 4) the inherent difference in the coordinate systems, or 5) the difference between C_{n_r} and $(C_{M_q} + C_{M_{\dot{\alpha}}})$. However, it can be shown that the difference corresponds to magnitude $\psi' \epsilon'$.

The inertial terms in both the Euler angle equations, derived herein, and the transformed exact aeroballistic equations are identical. It is important to note that agreement between the trigonometric form of the inertial terms depends only upon retaining the β terms in equation 29). The effect of including $\hat{\nu}$ in equation 29) is a modification of the θ' terms in equations 30) and 31), namely, θ' is everywhere replaced by $(\theta' + \hat{\nu})$. Although the form of the transformed aeroballistic equations is not affected by $\hat{\nu}$, it is clear that for any comparison with observed motions, $\hat{\nu}$ must be included. This would also include analysis of experimental data.

IV. AERODYNAMIC MOMENT EXPANSIONS

General

With the new fixed-plane equations of motion in polar form the aerodynamic moments M and N are related directly to the angle of attack and Magnus planes, and each appears in only one equation. This division of the aerodynamic system will be fully exploited.

Of particular concern is the appropriate formulation of what might be called dynamic Magnus effect. This is the contribution to N resulting from angle of attack plane rotation. This dynamic Magnus effect must be considered for finite as well as zero spin, since it is not at all clear that the effect of angle of attack plane rotation disappears for zero spin.

Although there is some concern about the most appropriate means of describing an aerodynamic system in analytic terms,* both precedent and convenience leads us to consider, at least initially, a series expansion scheme in terms of the variables appearing in the equation of motion. Independently, we examine both theoretically and empirically the aerodynamic force structure on bodies of interest to confirm the suitability of the aerodynamic model. It is important to realize that certain pitfalls exist when one tries to combine a theoretically derived model of the complete aerodynamic system with certain conjectures as to the form of specific aerodynamic effects. This point will be brought out more fully when we consider the effect of n-gonal rotational symmetry.

Maple-Synge Theory

The systematic development of the aerodynamic force system for projectiles,including the effects of rotational and reflectional symmetry, is due

* Tobak and Etkin have both suggested alternate formulations of the aerodynamic force system.

principally to the work of Maple and Synge, ref. 8. The basic hypothesis involved in their analysis is that the acrodynamic force system depends upon the instantaneous motion of the body. The two specific types of symmetry considered are, 1) n-gonal rotational symmetry about an axis, A, 2) reflectional symmetry in a plane, P. The precise application of the Maple-Synge theory depends upon the choice variables used to describe the motion, but in any case, the end result is basically the same, viz., the theory shows which of the coefficients of the expansion remain after certain "covering operations" are performed. The coefficients thus eliminated are inconsistent with the covering operations. For n-gonal symmetry this whole process amounts to forming a coefficient-eliminating sieve. The sieve can be expressed in the form of a diagram, which shows the surviving coefficients of each degree in terms of two parameters. A different sieve is constructed for the transverse and axial modes, and for each type of rotational symmetry.

Using the Maple-Synge theory directly, the variables are the complex cross velocity and the comples cross angular velocity. These are used in their equivalent form, $u, \bar{u}, \omega$ and $\bar{\omega}$. It is understood that the coefficients are also function of the axial velocity and spin as well as air density, etc.

The appropriate coefficients for n-gonal rotational symmetry are provided by Maple & Synge in a convenient form in ref. 8, and hence their development will not be repeated here. The development can be extended to derivatives of the variables as well as the variables themselves.

The consequences of mirror symmetry, however, will be considered briefly, as this analysis leads to different results depending upon the choice of variables. This point is brought home by the way of an example in Appendix A. Thus, the Maple-Synge rules regarding terms which vanish for mirror symmetry, cannot be used in a general sense, and apply only to the Maple-Synge variables. When $\xi, \bar{\xi}, \xi', \bar{\xi}'$ are used as variables, a new set of rules must be developed.

Since the present effort is of an exploratory nature, the aerodynamic expansion will be developed for just a representative case. We shall arbitrarily choose a body with tetragonal rotational symmetry and mirror symmetry, and we shall further assume that coefficients up to and including cubic terms are sufficient to describe the aerodynamic system. For other types of symmetry and for higher order terms in the aerodynamic expansion, the development will be much the same.

For the case considered, we obtain the following Maple-Synge moment coefficients for the transverse axes:

$$G_{1000}(u) = (g_{01}p + ig_{02})u$$

$$G_{0010}(\omega) = (g_{03} + ipg_{04})\omega$$

$$G_{2100}(u^2, \bar{u}) = (g_1 p + ig_2)u^2\bar{u}$$

$$G_{1110}(u, \bar{u}, \omega) = (g_3 + ipg_4)u\bar{u}\omega$$

$$G_{0120}(\bar{u}, \omega^2) = (g_5 p + ig_6)\bar{u}\omega^2$$

$$G_{2001}(u^2, \bar{\omega}) = (g_7 + ipg_8)u^2\bar{\omega}$$

$$G_{1011}(u, \omega, \bar{\omega}) = (g_9 p + ig_{10})u\omega\bar{\omega}$$

$$G_{0021}(\omega^2, \bar{\omega}) = (g_{11} + ipg_{12})\omega^2\bar{\omega}$$

$$G_{0300}(\bar{u}^3) = (g_{13}p + ig_{14})\bar{u}^3$$

$$G_{0201}(\bar{u}^2, \bar{\omega}) = (g_{15} + ig_{16}p)\bar{u}^2\bar{\omega}$$

$$G_{0102}(\bar{u}, \bar{\omega}^2) = (g_{17}p + ig_{18})\bar{u}\bar{\omega}^2$$

$$G_{0003}(\bar{\omega}^3) = (g_{19} + ipg_{20})\bar{\omega}^3$$

It can be shown that the first six pair of cubic coefficients are applicable to a body of revolution, while the last four pair of coefficients, g_{13} through g_{20}, are a consequence of the tetragonal symmetry.

Transformation of Maple-Synge Coefficients to Fixed-Plane Axes

The above coefficients are derived on the basis of body-fixed axes. We must therefore consider the correct formulation for fixed-plane axes, aligned with the angle of attack plane and Magnus plane.

The relationship between $M + i N$, where M is the moment in the angle of attack plane and N is the moment in the Magnus plane, and the Maple-Synge $G = G_1 + i G_2$ is obtained from the following sketch:

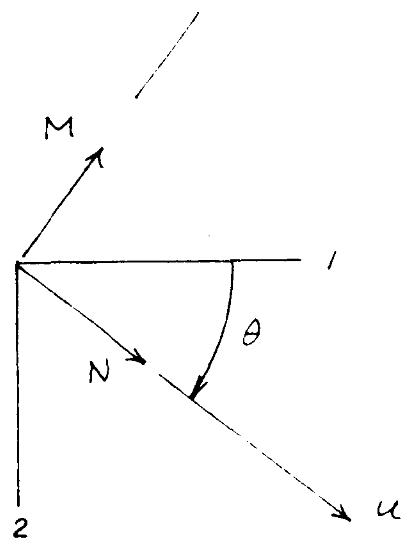

The resulting equation relating these two sets of moments is

$$G = G_1 + i G_2 = -i e^{i\theta}(M + iN) \tag{35}$$

We may also define $u = S e^{i\theta}$, from which we obtain immediately

$$\bar{u} = S e^{-i\theta}$$
$$u\bar{u} = S^2$$

The relationship between angular velocities in the two systems is given by the following sketch:

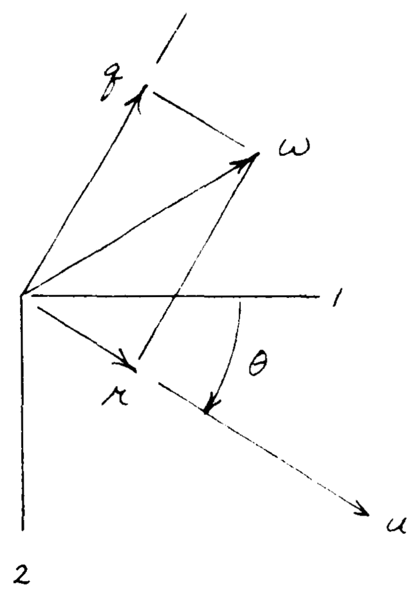

We obtain that

$$\omega = e^{i\theta}(r - iq)$$
$$\bar{\omega} = e^{-i\theta}(r + iq)$$

First we will consider the effect of the above relationships on a linear term, as follows:

$$G_{1000}(u) = (g_{01}p + ig_{02})u = -ie^{i\theta}(M+iN)_{1000}$$

$$(g_{01}p + ig_{02})\delta e^{i\theta} = -ie^{i\theta}(M+iN)_{1000}$$

From this it is clear that

$$M_\delta \delta = -g_{02}\delta$$

$$N_{p\delta} p\delta = g_{01} p\delta$$

Similarly, we obtain for the other linear coefficients

$$G_{0010}(\omega) = (g_{03} + ipg_{04})\omega = -ie^{i\theta}(M+iN)_{0010}$$

$$(g_{03} + ipg_{04})e^{i\theta}(r - iq) = -ie^{i\theta}(M+iN)_{0010}$$

from which we see that

$$g_{03} = N_r = M_q$$

$$g_{04} = -M_{pr} = N_{pq}$$

Cubic Coefficients - Body of Revolution

A typical transformation of the first six pair of cubic terms is given next. Consider the term

$$G_{1110}(u, \bar{u}, \omega) = (g_3 + ipg_4)u\bar{u}\omega$$

From our basic relationships:

$$(g_3 + ipg_4)\delta^2(r - iq)e^{i\theta} = -ie^{i\theta}(M+iN)_{1110}$$

$$[(g_3 q - g_4 pr) + i(g_3 r + g_4 pq)]\delta^2 = \delta^2(M_{\delta^2} + iN_{\delta^2})_{1110}$$

therefore,

$$g_3 = (M_{\delta^2 q})_{1110} = (N_{\delta^2 r})_{1110}$$

$$g_4 = (M_{\delta^2 pr})_{1110} = (-N_{\delta^2 pq})_{1110}$$

The Maple-Synge indices are retained here because different Maple-Synge cubic terms may lead to the same fixed-plane coefficient. For example, from G_{2001}, we obtain

$$g_7 = (-M_{\delta^2 q})_{2001} = (N_{\delta^2 r})_{2001}$$

$$g_8 = (-M_{\delta^2 pr})_{2001} = (-N_{\delta^2 pq})_{2001}$$

The transformations for the first six cubic coefficients are summarized in the following table:

G_{2100} :	$g_2 = -M_{\delta^3}$		$g_1 = N_{p\delta^3}$
G_{1110} :	$g_3 = M_{\delta^2 q} = N_{\delta^2 r}$		$g_4 = -M_{\delta^2 pr} = N_{\delta^2 pq}$
G_{0120} :	$g_6 = -M_{\delta(r^2+q^2)} = \frac{1}{2} N_{\delta rq}$		$g_5 = \frac{1}{2} M_{\delta pqr} = N_{\delta p(r^2+q^2)}$
G_{2001} :	$g_7 = -M_{\delta^2 q} = N_{\delta^2 r}$		$g_8 = -M_{\delta^2 pr} = -N_{\delta^2 pq}$
G_{1011} :	$g_{10} = -M_{\delta(r^2+q^2)}$		$g_9 = N_{\delta(r^2+q^2)p}$
G_{0021} :	$g_{11} = M_{q(q^2+r^2)} = N_{r(q^2+r^2)}$		$g_{12} = -M_{pr(r^2+q^2)} = N_{pq(r^2+q^2)}$

For the zero spin case we can conveniently compare the Maple-Synge, fixed-plane, and Murphy coefficients from BRL Rpt. 1071. These are given in the Table below:

Cubic Coefficients For
Body of Revolution
with Zero Spin

Maple-Synge Coefficients	Fixed-Plane Coefficients for Angle of Attack & Magnus Planes	Murphy Coefficients
$-g_2$	M_{δ^3}	M_{100}
$g_3 - g_7$	$M_{\delta^2\xi}$	$M_{010} - H_{100}$
$-g_6 - g_{10}$	$M_{\delta\lambda^2}$, $M_{\delta\xi^2}$, $M_{\delta(\lambda^2+\xi^2)}$	$M_{001} + H_{010}$
g_{11}	$M_{\xi^3} + M_{\xi\lambda^2}$	$-H_{001}$
$g_3 + g_7$	$N_{\delta^2\lambda}$	$-H_{100} - M_{010}$
$2g_6$	$N_{\delta\lambda\xi}$	$-2H_{010}$
g_{11}	$N_{\lambda\xi^2}$, N_{λ^3}, $N_{\lambda(\lambda^2+\xi^2)}$	$-H_{001}$

It is of interest, that only six independent cubic coefficients remain. Also, it will be noted that the Murphy and Maple-Synge coefficients are identical, except for the signs of certain coefficients.

The advantage of the fixed-plane coefficients, at this point, lies in their direct relationship to those physical parameters of the motion which are easily measured. For example, both wind tunnel and free-flight instrumentation systems are available which can easily separate the angular velocity components with respect to the angle of attack plane. On the other hand, the direct measurement of the complex-conjugate variables would be extremely difficult.

The dynamic Magnus effect, due to angle of attack plane rotation, is also well described by the fixed-plane cubic coefficients. At zero spin we have $N_{\delta^2 r}$, $N_{\delta r q}$, $N_{r q^2}$ and N_{r^3} contributions in the Magnus plane and of these $N_{\delta^2 r}$ and N_{r^3} contribute to pure circular motions. With axial spin included, we add $N_{p\delta(r^2+q^2)}$ and $N_{pq(r^2+q^2)}$ contributions to the Magnus plane. The former also contributes to pure circular motion.

Cubic Coefficients - Tetragonal Rotational Symmetry

In the preceding transformations for the cubic body-of-revolution terms, the $e^{i\theta}$ factor always appeared on both the left and right sides of the equation, thus cancelling out. The last four cubic terms for a body with tetragonal rotational symmetry (G_{0300}, G_{0201}, and G_{0003}) do not behave in the same manner. Consider, for example, the term $G_{0300}(\bar{u}^3)$. Proceeding as before, we let

$$(g_{13}\, p + i\, g_{14})\,\bar{u}^3 = -i\, e^{i\theta}(M + iN)_{0300}$$

$$(g_{13}\, p + i\, g_{14})\,\delta^3 e^{-3i\theta} = -i\, e^{i\theta}(M + iN)_{0300}$$

The form of the latter equation suggests a re-arrangement to

$$(g_{13}\, p + i\, g_{14})\,\delta^3 = (\cos 4\theta + i \sin 4\theta)(N_{\delta^3} - i M_{\delta^3})_{0300}$$

in which case we obtain:

$$g_{14} = -M_{\delta^3} \cos 4\theta + N_{\delta^3} \sin 4\theta$$

$$g_{13} = M_{\delta^3 p} \sin 4\theta + N_{\delta^3 p} \cos 4\theta$$

Thus g_{13} and g_{14} actually represent coefficients which are periodic in the aerodynamic roll angle, since θ is precisely the angle between an arbitrary set of body-fixed axes and the angle of attack plane. The relationships for g_{13} and g_{14} can be made very precise, by letting the body-fixed axes be aligned with the fin planes.

At this point we certainly see the validity of our earlier remarks regarding a composite aerodynamic formulation, viz, a combination theoretical and empirical aerodynamic model. For it could have been possible to introduce both $G_{0300}(\bar{u}^3)$ and terms like

$$M = k(1 + \cos n\theta)\delta^3$$

without realizing their equivalence. This particular problem has also been discussed by Zaroodny, ref. 10.

The remaining cubic terms (G_{0201}, G_{0102}, and G_{0003}), become increasingly complicated when transformed to the angle of attack and Magnus planes, and will not be presented here. Also, unique spin dependent terms cannot be separated. For zero spin we obtain

$$g_{15} = N_{\delta^2 r} \cos 4\theta + M_{\delta^2 r} \sin 4\theta$$

or $$g_{15} = N_{\delta^2 q} \sin 4\theta - M_{\delta^2 q} \cos 4\theta$$

$$g_{18} = \tfrac{1}{2}\left[N_{\delta r q} \cos 4\theta + M_{\delta r q} \sin 4\theta \right]$$

or $$g_{18} = N_{\delta(r^2 - q^2)} \sin 4\theta - M_{\delta(r^2 - q^2)} \cos 4\theta$$

$$g_{19} = N_{(r^3 - 3rq^2)} \cos 4\theta + M_{(r^3 - 3rq^2)} \sin 4\theta$$

or $$g_{19} = N_{(3qr^2 - q^3)} \sin 4\theta - M_{(3qr^2 - q^3)} \cos 4\theta$$

In essence, the last three G coefficients merely state that the dynamic Magnus effect is periodic in roll. From a practical viewpoint, as Zaroodny points out in ref. 10, it makes more sense to use higher order terms in δ, than to retain angular velocity coefficients like G_{0102} ($\nu \bar{\omega}^2$) and G_{0003} ($\bar{\omega}^3$). This is because the angular velocity coefficients contribute smaller aerodynamic moments than do the coefficients depending upon angle of attack.

With our clear understanding of the physical significance of the Maple-Synge terms, we can at last allow additional non-Maple-Synge terms to be considered. Such a candidate term could be ν_δ, and the variation of ν_δ with aerodynamic roll angle. However, terms such as this should only be considered when sufficient experimental data are available to establish their validity. In practice, the ν_{δ^2} term contained in the Maple-Synge scheme, may alone provide a sufficient representation of the experimental data. This is because it is often difficult to obtain precise aerodynamic measurements at very small angles of attack.

V. APPLICATION OF PERTUBATION THEORY TO NEAR-CIRCULAR MOTIONS

A. A Test Case for Comparison with Quasi-Linear Theory

The general validity of the small pertubation approach for analysis of circular motions has been established by Haseltine.[5] However, from his general analysis it is not at all clear how the stability requirements will be expressed for specific nonlinear differential equations.

To establish a firm basis for the pertubation approach, a specific set of nonlinear differential equations for zero spin and cubic aerodynamic coefficients are analyzed. Murphy has obtained a quasi-linear solution to these equations and has established the stability requirements with respect to the amplitude plane.[9] We will develop a corresponding solution and stability requirements by first writing the equations of motion in polar form, and then developing small pertubation equations for near-circular motion. The Routh stability criteria will then be applied to the characteristic equation describing the pertubation equations.

This exercise will also serve to illustrate some of the differences between the complex-variable and the polar equations.

The basic differential equation in complex variables is:

$$\xi'' - M_o \xi = -H\xi' + (M - M_o)\xi \qquad 36)$$

where

$$M = M_o + M_{100}\xi\bar{\xi} + M_{010}\xi\bar{\xi}' + M_{001}\xi'\bar{\xi}'$$

$$H = H_o + H_{100}\xi\bar{\xi} + H_{010}\bar{\xi}\xi' + H_{001}\xi'\bar{\xi}'$$

The corresponding polar equations, with $\xi = \delta e^{i\theta}$, are

$$\delta'' - \delta(\theta')^2 + H_0\delta' + H_{100}\delta^2\delta' + H_{010}\delta(\delta')^2 - H_{010}\delta(\delta\theta')^2 + H_{001}(\delta')^3 + H_{001}\delta'(\delta\theta')^2 - M_0\delta - M_{100}\delta^3 - M_{010}\delta^2\delta' - M_{001}\delta(\delta')^2 - M_{001}\delta(\delta\theta')^2 = 0 \qquad 37)$$

$$2\delta'\theta' + \theta''\delta + H_0\delta\theta' + H_{100}\delta^2(\delta\theta') + 2H_{010}\delta\delta'(\delta\theta') + H_{001}(\delta')^2\delta\theta' + H_{001}(\delta\theta')^3 + M_{010}\delta^2(\delta\theta') = 0 \qquad 38)$$

One of the disadvantages of the Murphy cubic coefficients is evident from equations 37) and 38), namely, that more than one aerodynamic coefficient exists for the same motion parameter. Specifically it is seen from equation 37) that H_{010} and M_{001} are both coefficients of $\delta(\delta')^2$ and that H_{100} and M_{010} are both coefficients of $\delta^2(\delta')$. Also in equation 38) both H_{100} and M_{010} are coefficients of $\delta^2(\delta\theta')$.

To form pertubation equations from 37) and 38) we assume that the motion will be near-circular so that we can replace δ and θ' by

$$\delta = \delta_0 + \Delta\delta \qquad 39)$$
$$\theta' = \theta_0' + \Delta\theta'$$

Following the usual procedure, equations 39) are substituted into 37) and 38) and second order and smaller terms in $\Delta\delta$ and $\Delta\theta'$ are neglected. We then obtain, after some rearranging, two linear differential equations in $\Delta\delta$ and $\Delta\theta'$. These equations are presented below in operator form, where $\mathcal{D} = \frac{d(\ )}{ds}$, and s is the independent variable.

$$\Big[D^2 + (\theta_0')^2 + H_0 D + H_{100}\delta_0^2 D - 3H_{010}(\delta_0\theta_0')^2 + H_{001}(\delta_0\theta_0')^2 D - M_0 - 3M_{100}\delta_0^2 - M_{010}\delta_0^2 D - 3M_{001}(\delta_0\theta_0')^2 \Big]\Delta\delta + \Big[-2\delta_0\theta_0' - 2H_{010}\delta_0^3\theta_0' - 2M_{001}\delta_0^3\theta_0' \Big]\Delta\theta' = \delta_0(\theta_0')^2 + H_{010}\delta_0(\delta_0\theta_0')^2 + M_0\delta_0 + M_{100}\delta_0^3 + M_{001}\delta_0(\delta_0\theta_0')^2 \qquad 40)$$

$$\Big[2\theta_0' D + H_0\theta_0' + 3H_{100}\delta_0^2\theta_0' + 2H_{010}\delta_0^2\theta_0' D + 3H_{001}(\delta_0\theta_0')^2\theta_0' + 3M_{010}\delta_0^2\theta_0' \Big]\Delta\delta + \Big[\delta_0 D + H_0\delta_0 + H_{100}\delta_0^3 + 3H_{001}(\delta_0\theta_0')^2\delta_0 + M_{010}\delta_0^3 \Big]\Delta\theta' = -H_0\delta_0\theta_0' - H_{100}\delta_0^2(\delta_0\theta_0') - H_{001}(\delta_0\theta_0')^3 - M_{010}(\delta_0\theta_0')\delta_0^2 \qquad 41)$$

From the nonhomogeneous part of equations 40) and 41) we readily obtain a steady-state circular motion amplitude, δ_0, and the circular motion rate, θ_0'. These are given by

$$\delta_0^2 = \frac{-H_{000}}{M_{010} + H_{100} - M_0 H_{001} + (H_0 H_{010} + M_{001} H_0)} \qquad 42)$$

and

$$(\theta_0')^2 = -M_0 + H_0\left(\frac{H_{010}}{H_{001}} + \frac{M_{001}}{H_{001}}\right) \qquad 43)$$

The frequency θ_0' is very close to the natural pitch frequency, and supports the assumptions used by Murphy in the quasi-linear method. The amplitude, with the exception of the small term in the brackets in equation 42), is identical to Murphy's result.

The homogeneous part of equations 40) and 41) leads to a third order characteristic equation of the form

$$A\lambda^3 + B\lambda^2 + C\lambda + D = 0 \tag{44}$$

The stability of the system is governed by the nature of the roots. Routh has shown that the necessary and sufficient condition for stability (i.e., that no root of the equation shall be zero or have a positive real part), when the characteristic equation is cubic, are that A, B, D, and BC-AD be positive.

To generate these test functions we expand the determinant formed by the coefficients of $\Delta\vartheta$ and $\Delta\theta'$ in equations 40) and 41). The test functions can then be expressed entirely in terms of the aerodynamic and physical parameters by substituting equations 42) and 43) for ϑ_0 and θ_0'.

After some very lengthy algebra we find that

$$A = 1 \tag{45}$$

$$B = \frac{2H_0\left(M_{010} + H_{001}M_0\right)}{h} \tag{46}$$

$$C \approx -4M_0 \tag{47}$$

$$D \approx 4H_0 M_0 \tag{48}$$

$$BC\text{-}AD \approx \frac{-4 H_0 M_0 \left(H_{100} + 3 M_{010} + H_{001} M_0 \right)}{n} \qquad 49)$$

where $$n = M_{010} + H_{100} - M_0 H_{001} \qquad 50)$$

If it is assumed that the body is aerodynamically stable, i.e., $M_0 < 0$, then it follows from equations 42), 46), 48), 49) that the following inequalities must be satisfied.*

$$\begin{aligned} H_0 &< 0 \\ n &> 0 \\ H_{100} + 3 M_{010} + H_{001} M_0 &< 0 \\ M_{010} + H_{001} M_0 &> 0 \end{aligned} \qquad 51)$$

These are precisely the same stability criteria obtained by Murphy. These conditions can be illustrated by a stability diagram in the M_{010}, H_{100} plane as depicted below:

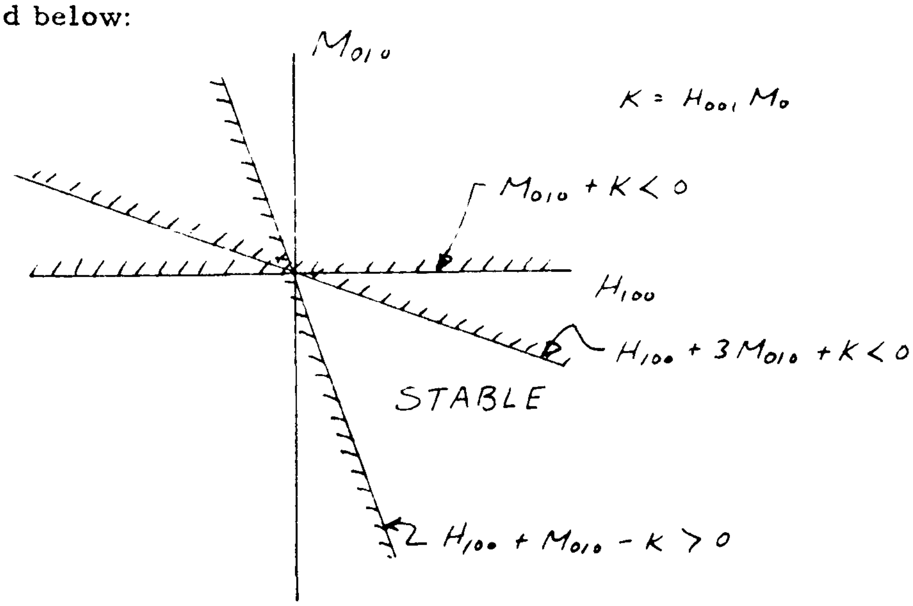

* Equation 42) must be satisfied such that $\delta_0^2 > 0$.

Thus, the small pertubation theory, applied to the polar equations of motion, obtains results which are consistent with the quasi-linear amplitude plane analysis of Murphy. However, in some respects, the present method is more advantageous. First, the pertubation method, as used here, is not as restricted as to the types of nonlinearities present in the equations of motion. Both aerodynamic and geometric nonlinearities can be handled, and the latter can be retained in trigonometric form if necessary. Second, the degree of approximation involved in the stability boundaries can be established more easily, since the relative magnitude of the terms in the coefficients of the characteristic equation can be determined, if necessary, by direct numerical analysis.

B. Cubic Static Moments and Modified Damping

We will now consider an aerodynamic system which is of practical interest, but yet not completely compatible with Maple-Synge. This particular case involves a cubic as well as linear side moment, the latter not being given by Maple-Synge. We shall also consider two different values for the damping, one value H_1, applicable to the polar equation corresponding to the real variables, and a second value, H_2, for the polar equation corresponding to the imaginary variables.

These new equations are

$$\vec{\alpha}'' + \frac{pd}{V}\frac{I_x}{I}\psi'\sin\vec{\alpha} - (\psi')^2\cos\vec{\alpha}\sin\vec{\alpha} - \frac{\rho S d^3}{2I}\left[C_{m_\alpha} + C_{m_2}\vec{\alpha}^2\right]\vec{\alpha} + H_1\vec{\alpha}' = 0 \tag{52}$$

$$\psi''\sin\vec{\alpha} - \frac{I_x}{I}\frac{pd}{V}\vec{\alpha}' + 2\psi'\vec{\alpha}'\cos\vec{\alpha} + H_2\psi'\sin\vec{\alpha} - \frac{\rho S d^3}{2I}\left[C_{n_\alpha} + C_{n_2}\vec{\alpha}^2\right]\vec{\alpha} - \frac{\rho S d^3}{2I}\left[C_{n_{p\alpha}} + C_{L_\alpha}\frac{I_x}{I}\right]\frac{pd}{V}\vec{\alpha} = 0 \tag{53}$$

The application of these equations, which include the side moment terms, arises most frequently where the motion is locked-in or lunar. In this case

$$\psi' = \frac{pd}{V} \Big/ \cos \vec{\alpha}$$

and equations 52) and 53) become

$$\vec{\alpha}'' - (\psi')^2 (\cos \vec{\alpha} \sin \vec{\alpha}) \left[1 - \frac{I_x}{I}\right] + H_1 \vec{\alpha}' - \frac{\rho s d^3}{2I} \left[C_{m_\alpha} + C_{m_2} \vec{\alpha}^2\right] \vec{\alpha} = 0 \qquad 54)$$

$$\psi'' \sin \vec{\alpha} + \psi' \vec{\alpha}' (\cos \vec{\alpha}) \left[2 - \frac{I_x}{I}\right] + H_2 \psi' \sin \vec{\alpha} - \frac{\rho s d^3}{2I} \left[C_{n_\alpha} + C_{n_2} \vec{\alpha}^2\right] \vec{\alpha} = 0 \qquad 55)$$

The steady-state circular motion solutions are given by the following two simultaneous equations:

$$-(\psi_o')^2 (\cos \vec{\alpha}_o \sin \vec{\alpha}_o) \left[1 - \frac{I_x}{I}\right] - \frac{\rho s d^3}{2I} \left[C_{m_\alpha} + C_{m_2} \vec{\alpha}_o^2\right] \vec{\alpha}_o = 0 \qquad 56)$$

$$H_2 (\psi_o') \sin \vec{\alpha}_o - \frac{\rho s d^3}{2I} \left[C_{n_\alpha} + C_{n_2} \vec{\alpha}_o^2\right] \vec{\alpha}_o = 0 \qquad 57)$$

Generally, for small values of $\vec{\alpha}_o$, only one real solution for ψ_o' will be obtained. The solution of 56) and 57) is shown qualitatively in the following sketch, for negative values of the C_m's and positive values of C_n's

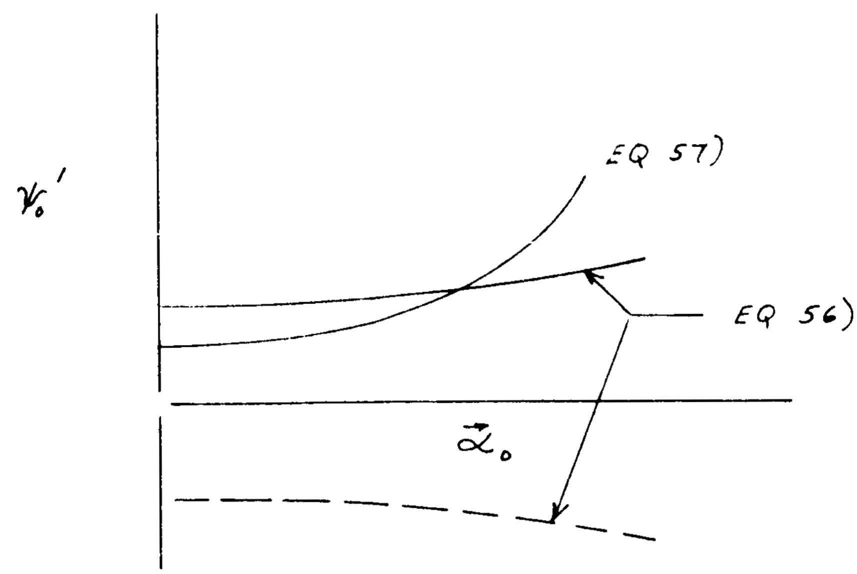

It might be noted that for a fifth order expansion of C_n, two circular motion solutions could be obtained. In the latter case, one solution would be stable and the other unstable.

A pertubation analysis of equations 54) and 55) can be accomplished by letting

$$\vec{\alpha} = \vec{\alpha}_0 + \Delta\vec{\alpha}$$
$$\psi' = \psi_0' + \Delta\psi' \qquad 58)$$

from which we also obtain

$$\cos\vec{\alpha} = \cos\vec{\alpha}_0 - \Delta\vec{\alpha}\sin\vec{\alpha}_0$$
$$\sin\vec{\alpha} = \sin\vec{\alpha}_0 + \Delta\vec{\alpha}\cos\vec{\alpha}_0 \qquad 59)$$

Substituting equations 58) and 59) into equation 54) and 55), expanding, deleting terms of second order and higher in $\Delta\vec{\alpha}$ and $\Delta\psi'$, we obtain a new set of linear differential equations whose characteristic function

$$A\lambda^3 + B\lambda^2 + C\lambda + D = 0$$

has the following coefficients

$$A = 1 \qquad 60)$$
$$B = H_1 + H_2$$
$$C = H_1H_2 + J + L\left(\psi_0'\cos\vec{\alpha}_0\right)\left(2 - I_x/I\right)$$
$$D = JH_2 + KL$$

where

$$J = \left\{ -\left(\psi_0'\right)^2\left(\cos 2\vec{\alpha}_0\right)\left(1 - \frac{I_x}{I}\right) - \left[\frac{C_{m_\alpha} + 3C_{m_2}\vec{\alpha}_0^2}{2I'}\right]\right\}$$

$$K = H_2 \psi_0' \cos\vec{\alpha}_0 - \left[\frac{C_{n_\alpha} + 3 C_{n_2} \vec{\alpha}_0^2}{2 I'} \right]$$

$$L = 2(\psi_0')(\cos\vec{\alpha}_0)\left(1 - \frac{I_x}{I}\right)$$

Since our interest lies with the stability of the linear pertubation equations in the neighborhood of the steady-state solution, we can obtain (ψ_0') from 56) and 57) and substitute the result into the coefficients of equations 60c) and 60d). Unfortunately, the remaining equations must contain $\vec{\alpha}_0$ implicitly. As a result we obtain

$$C = H_1 H_2 - \left[\frac{C_{m_\alpha} + 3 C_{m_2} \vec{\alpha}_0^2}{2 I'} \right] + \left[\left(\frac{C_{m_\alpha} + C_{m_2} \vec{\alpha}_0^2}{2 I'} \right) \left(\frac{\vec{\alpha}_0}{\sin\vec{\alpha}_0 \cos\vec{\alpha}_0} \right) \left(\cos 2\vec{\alpha}_0 - 2(\cos^2\vec{\alpha}_0)\left(2 - \frac{I_x}{I}\right) \right) \right] \qquad 61)$$

$$D = -H_2 \left\{ \left[\frac{C_{m_\alpha} + 3 C_{m_2} \vec{\alpha}_0^2}{2 I'} \right] + \left[\frac{(C_{n_\alpha} + 3 C_{n_2} \vec{\alpha}_0^2)(C_{n_\alpha} + C_{n_2} \vec{\alpha}_0^2)}{(2 I' H_2)^2} \right] \left[\left(1 - \frac{I_x}{I}\right) \left(\frac{2 \vec{\alpha}_0 \cos\vec{\alpha}_0}{\sin\vec{\alpha}_0} \right) \right] \right\} \qquad 62)$$

Good approximations for C and D at small $\vec{\alpha}_0$ are

$$C = -\frac{2 C_{m_\alpha}}{I'} - \frac{3 C_{m_2} \vec{\alpha}_0^2}{I'}$$

$$D = -H_2 \left\{ \left[\frac{C_{m_\alpha} + 3 C_{m_2} \vec{\alpha}_0^2}{2 I'} \right] + 2\left(1 - \frac{I_x}{I}\right) \frac{(C_{n_\alpha} + 3 C_{n_2} \vec{\alpha}_0^2)(C_{n_\alpha} + C_{n_2} \vec{\alpha}_0^2)}{(2 H_2 I')^2} \right\}$$

As before, the necessary and sufficient conditions for stability are that A, B, C, D and BC-AD be positive. For missiles with aerodynamic stability, $C_{m_\alpha} < 0$, and $H_1 > 0$, $H_2 > 0$, the circular motion solutions will be stable if C_{n_α} and the nonlinearities C_{m2} and C_{n2} are small. When $C_{m2} > 0$, and the total C_n contribution is large, both the C and D coefficients as well as BC-AD may become negative. It should also be noted that for $H_2 < 0$, the system can still be stable if $|H_1| > |H_2|$ and the total C_n is large, such that $D > 0$. Thus the circular motion damping, H_2, effects the stability in a different manner than the planar motion damping, H_1.

VI. AERODYNAMICS OF NEAR-CIRCULAR AND NON-PLANAR MOTION

General

A complete treatment of the aerodynamic phenomena associated with near-circular and non-planar motions is beyond the scope of the present contractural effort and this report. However, an understanding of the non-planar motion problem requires some insight of the aerodynamic factors involved. In particular, it is desirable to examine the source of the Magnus-type moments, which promote the angle of attack plane rotation. Also, we shall consider the nature of the cross-flow on inclined bodies of revolution, not only as it pertains to Magnus forces and moments, but also to higher order stability and/or damping coefficients. Finally, the state-of-the-art relative to the prediction and measurement of aerodynamic stability coefficients for non-planar motion will be reviewed.

The discussion which follows in this report is of a general nature. More specific work, related to the development of cross-flow theory for calculation of aerodynamic stability coefficients, is contained in a separate report by Ray Rodman,[32] consultant to Alpha Research, Inc., for Contract NAS-2-3426.

Cross-Flow Phenomena

Cross-flow theory, perhaps, provides the most useful concept for visualization of the effects of body motion and flow conditions on the aerodynamic force system. This is particularly true where viscous effects are of primary interest. If a realistic cross-flow picture or model can be devised, stability coefficients can be computed from it in a relatively straight forward manner. In contrast, much more effort is required to obtain stability coefficients if the complete body pressure distribution must be determined. The extent to which the cross-flow can be considered independent of the axial flow requires careful consideration. This point will be emphasized in the discussions which follow.

The combining of aerodynamic potential and viscous flow forces and the super-position of body motions is basic to much of aerodynamics, and is the basis of cross-flow theory. Following the demonstration by R. T. Jones that in the case of laminar flow the viscous effects on a long yawed cylinder could be treated by considering the flow across the cylinder axis independently of the axial flow, Julian Allen proposed a cross-flow theory for bodies of revolution.[11] The basis for Allen's cross-flow theory is the use of a steady-state cross-flow drag coefficient for simulation of the viscous effect. Later work by H. Kelly[12] considers the impulsive nature of the cross-flow as well as the effect of a turbulent boundary layer. The Kelly theory leads to an odd polynominal for the body total cross force, a result which is in agreement with the Maple-Synge theory. A further improvement of Kelly's work is presently being accomplished by Rodman as part of the present effort.

To provide a more firm basis for the cross-flow theory, flow visualization and other tests have been conducted by a number of researchers.[13, 14, 15.] A number of significant discrepancies with the ideal cross-flow postulation have been observed, particularly where the boundary layer is in a transitional state or affected by compressibility. These flow visualization studies, such as the work of Allen and Perkins[13] began to show the importance, also, of the wake and vortex structure in the lee of the body.

Somewhat independently, Eldon Dunn,[16] and William Letko[17] reported anomalous side force characteristics for bodies of revolution at large angles of attack with zero sideslip. These results were also traced to asymmetric vortex formation.

Closer study of the flow around pointed bodies of revolution at angle of attack has shown that at least three different types of vortex formation can occur behind the body; steady symmetric, steady asymmetric, and unsteady asymmetric. Curry and Reed[18] have found both the steady symmetric and steady asymmetric formation appearing with a sounding rocket model both with and without axial spin. Their results also show hysteresis effects associated with large variations in the angle of attack. Recent vapor screen experiments by Tobak and Peterson at the NASA Ames Research Center have shown the steady asymmetric vortex formation occuring with a body of revolution in a lunar coning motion.* Of considerable interest is the work of Thompson and Morrison,[19] which includes both experimental and theoretical treatment of the steady-asymmetric vortex case. Their flow model, which is restricted to sub-critical cross-flow Reynolds numbers, incorporates vortex shedding from alternate sides of the body in a manner related to the Karman vortex street formation. In the Thomson-Morrison theory, the Strouhal number becomes an important similarity parameter.

The angle of attack range corresponding to the various vortex and wake formations is of practical interest, since most missiles are designed to fly at small or moderate angles of attack. The following discussion is restricted to long slender bodies. Of first interest is the angle at which flow separation begins, since it is within this separated-flow region that the vortices are formed. The initial cross-flow separation has a boundary not unlike that of the minimum pressure line, where it will be recalled that for pointed nose bodies at angle of attack the most forward point on the minimum-pressure line is aft of the nose. In general, separation will start at the most aft portion of

---

* These experiments also show that the angular displacement of the vortices with respect to the angle of attack plane varies along the length of the body. Such an effect will lead to very nonlinear damping moments.

the body and move forward towards the minimum-pressure line. The longitudinal position at which cross-flow separation first occurs at various angles of attack has been determined by Perkins and Kuehn.[15] At Mach number 1.98 it was found that separation began at angle of attack as small as one degree at a point 11 diameters aft of the nose.

As the angle of attack is increased, there is first formed a pair of symmetrical vortices and at subcritical cross-flow Reynolds numbers these subsequently break down into steady or unsteady asymmetrical vortices at higher angles of attack. The nature of the vortices at moderate angles of attack, i.e., 10-15 degrees,can be determined not only by flow observations, but also be pressure distribution data, side force measurements, and rolling moment characteristics (if the model has fins)

The side force measurements show that the steady asymmetrical vortices begin to form at from 15-20 degrees angle of attack at subsonic velocities.[16,17] The asymmetrical vortices form at the lowest angle for bodies with long pointed noses; the asymmetrical vortices are formed at a higher angle of attack if the nose length is short and conical. At low supersonic Mach numbers, asymmetrical rolling moments (indicative of asymmetric vortex formation) have been noted at about 10 degrees angle of attack.[19] At a Mach number of five, asymmetric side force characteristics are noted to commence at angles of attack as small as 2 degrees for a sounding rocket model.[18]

All of the above phenomena will influence the body non-planar motion. Murphy has shown that the cross-flow theory of Kelly, which assumes a symmetric wake, leads to values for all of the cubic damping coefficients for a body of revolution with zero spin. Thus, the more complicated cross-flows, such as those with asymmetric vortices, will probably make the aerodynamic force system even more nonlinear.

It is to be noted that the cross-flow characteristics at and above the angles of attack where flow separation begins, become extremely sensitive to the boundary-layer condition. The boundary layer in turn is sensitive to Reynolds number, Mach number, nose shape, body fineness ratio, and such geometric factors as roughness or protuberances. In addition the body motion; particularly spin and possibly coning, will influence the boundary layer. Thus, the cross-flow concept requires much additional evaluation before it can be fully exploited as a means of arriving at stability coefficients.

Magnus Phenomenon

Although the cross-flow concept is considered primarily in conjunction with the force distribution in the angle of attack plane, of equal importance are the effects in the Magnus plane. In fact, the classical Magnus force and moment (due to axial spin) for a body of revolution at angle of attack, can be developed along lines similar to the normal force and pitching moment, by replacing the cross drag coefficient with the Magnus force coefficient for a cylinder in cross-flow. The two-dimensional Magnus force characteristics of cylinders are quite well known. Both this approach and the somewhat more fundamental boundary-layer displacement theory of Kelly,[20] are adaptable to prediction of Magnus coefficients for non-planar motions.

Magnus-type moments are of interest from the standpoint that they provide a means for driving or sustaining non-planar or near-circular motions. For aerodynamically stable missiles, negative Magnus moments (with positive spin) are slightly more effective than positive moments in causing large angle of attack circular motions. However, lunar circular motions can occur only with positive Magnus moments since the angle of attack plane rotation must be in the same direction as the spin.

The classical Magnus force due to spin, can be either positive or negative, depending upon the cross-flow Reynolds number. This characteristic has been discussed by Krahn[21].

In recent years it has been recognized that there are sources for Magnus-type forces and moments in addition to the classical Magnus effect due to spin and the forces due to vortex asymmetry. These psuedo-Magnus forces are in most instances associated with finned missiles and occur even at relatively small spin rates. Several Magnus moment producing mechanisms, including body-fin interference,and differential fin cant, are described by Platau.[22]

Another type of Magnus force and moment occurs on finned vehicle when the fins are not aligned symmetrically with respect to the angle of attack plane. The body vortices apparently contribute the unsymmetrical flow field over the fins, but the complete process is not well understood and existing predictions are not in close agreement with experimental data. As discussed in an earlier section of the report, these forces and moments which are periodic in the aerodynamic roll angle, are for the most part consistent with the higher order Maple-Synge coefficients for bodies with n-gonal rotational symmetry.

Prediction of Stability Coefficients

From a dynamical point of view, our aerodynamic interest begins with the stability coefficients themselves, rather than with the details of the force distribution.

The prediction of the stability coefficients from cross-flow characteristics has been previously mentioned. This approach should be quite satisfactory for very large angles of attack, but may not be suitable for angles of attack approaching zero. It can be mentioned here, that the cross-flow theory clearly shows a difference between the damping in and normal to the angle of attack plane. In reference 1, it is shown that this difference approaches a factor of 2.0 at ninety degrees angle of attack.

At supersonic and hypersonic Mach numbers, several flow theories are available from which aerodynamic stability coefficients can be calculated. Although much work has been done to determine the stability coefficients for bodies of revolution from theory (see for example, references 23, 24, 25 and 26), the results to date have been obtained only for planar motions. It is envisioned that considerable effort will be required to calculate the nonlinear effects due to angle of attack plane rotation.

In regard to theoretical analysis of non-planar motions, it must be pointed out that the method used must be quite exact, otherwise identical results are likely to be obtained for both the planar and non-planar cases. Tobak and Lessing,[27] have noted that potential theory leads to coefficients for bodies of revolution which are unaffected by combined motions. Brunk[28] has noted that a simple analysis of the fin damping contribution leads to identical results for circular and planar motions.

Non-Planar Motion Experiments

It is significant that as yet there haven't been wind-tunnel measurements of the high order non-planar damping coefficients. In addition, nearly all wind-tunnel Magnus force and moment data have been obtained with the angle-of-attack plane fixed. Free-flight data have not been obtained in sufficient quantity or with sufficient accuracy to allow the determination of non-planar motion damping coefficients, or dynamic Magnus effect.

The only known force and moment measurements on bodies of revolution in pure circular motion are the results of reference 29. In these tests cone cylinder models were attached to a rotating sting, and a rotating force balance was utilized to measure the loads. The data indicates sizeable Magnus effect due to angle of attack plane rotation, in some cases sufficient to cause auto-rotation. A problem with such tests is the lack of force-balance sensitivity in the Magnus plane and the data degradation due to the use of slip-rings. Balances of new design are presently being fabricated, which have increased Magnus force sensitivity. When these are adapted to rotating sting support systems, it will finally be possible to make direct measurements of non-planar motion coefficients with some degree of accuracy.

Aerodynamic data for non-planar motions must at present be derived primarily from dynamic wind tunnel tests of bodies with two or three degrees of rotational freedom, such as those described in ref. 30. In general, insufficient data are obtained to separate the effects of spin and angle of attack plane rotation. The importance of varying the axial spin and angle of attack plane rotation independently cannot be overemphasized, both from the standpoint of providing simulation of the various free-flight motions, and also to allow the spin dependent Magnus effect to be isolated from the circular motion damping.

Another method of testing, which has been used for non-planar motion ayalysis, involves the use of a wind tunnel with rotating flow. Such a tunnel was at one time utilized by the NASA Langley Research Center. Test results obtained in this tunnel for a finned rocket model are described in ref. 21. These results are noteworthy in that they show the effect of modifications to the rocket nose, such as spoilers and arming propeller. The corresponding variations in the side moment at large angles of attack were found to be sufficient to cause limit circular motions at angles ranging from 30-40 degrees.

Determination of Stability Coefficients from Experimental Data

The basic problem of determining the nonlinear damping and Magnus coefficients which are associated with non-planar motions, is the achievement of sufficient variation in the motion parameters to isolate the separate effects of angle of attack, axial spin, and angle of attack plane rotation. Even for pure circular motion we must have sufficient data to determine at least the following Magnus-plane coefficients: N_{r} , $N_{p\delta}$, $N_{\delta^2 r}$, N_{r^3} , $N_{p\delta^3}$, $N_{p\delta r^2}$ and possibly $N_{\delta^3}(\theta)$, $N_{\delta^2 r}(\theta)$ etc. Some of these, such as $N_{p\delta}$, $N_{p\delta^3}$ and $N'_{\delta^3}(\theta)$ can be obtained without angle of attack plane rotation, but for analysis of general motions these static coefficients must be known for the appropriate range of Reynolds number, Mach number, etc. This means that, in general, both static and dynamic tests will have to be conducted as part of the same program.

There appears to be two methods of determining the coefficients which are dependent upon r; the first method involves the use of a rotating force balance, in the second method the coefficients would be inferred from the variation of r with time. The latter type test is possible if there is a driving moment opposite in sign to the damping moment at $r = 0$. This approach is analagous to the determination of the roll driving and damping coefficients by observation of the axial spin build-up from zero to steady-state.

VII. RECOMMENDATIONS FOR CIRCULAR MOTION EXPERIMENTS

Considerable information has been gathered as to the nature of the flow around bodies at angle of attack for conditions where the angle of attack plane is fixed. However, there is minimal experimental evidence to reveal how the flow and aerodynamic forces will be modified by angle of attack plane rotation. On the one hand, there is the possibility that the very sensitive separated flow regions, which are easily disrupted by small changes in the model or boundary-layer symmetry, may be stabilized by the presence of a quasi-steady circular motion. On the other hand, the change in the flow field around the body due to the circular motion, may itself initiate new and unique aerodynamic force distributions. One of the most important questions to be answered is whether the effects of circular motion can be isolated and superimposed on the results for the fixed angle of attack plane case. If so, a major extension of the cross-flow theory will be possible, namely, the prediction of aerodynamic coefficients for non-planar motion.

These and other questions regarding the effect of circular motion require two areas of study: 1) an examination and comparison of the local flow characteristics around models in circular motion as compared to results obtained with the angle of attack plane fixed; 2) investigation of the integrated effect of the circular motion on the total aerodynamic forces, moments, and stability coefficients. A complication to the study of circular motion is the separation of the effects of axial spin and angle-of-attack plane rotation. In any experimental program, means must be provided to vary the axial spin and the circular motion independently.

Direct Force Measurements

At the present time, the NASA Ames Research Center is preparing a model and model support system which will permit simultaneous axial spin and coning motion at fixed angles of attack. The system utilizes a rotating sting, with various adapters to achieve the desired angles of attack. The axial spin is provided by an electric motor attached to the sting. The model is being equipped with an internal force balance to permit direct measurement of the aerodynamic forces and moments in and normal to the angle of attack plane.

The above model installation can also be used for flow observations, particularly photographic observations of the flow relative to the angle of attack plane. This type data can be obtained with cameras attached to the rotating sting. Preliminary tests of this type have already been accomplished using the vapor screen technique, but only lunar motions have been investigated thus far.

Dynamic Model Tests with Free-Coning Motions

In many instances, the cost of a rotating balance will not be justifiable. An indirect method of measuring the moments in the Magnus plane, with and without angle of attack plane rotation, is therefore proposed.

A model supported at a fixed angle of attack by a freely-rotating sting,* as in the following sketch, will experience a rotational acceleration about the sting axis if there is a moment in the Magnus plane.

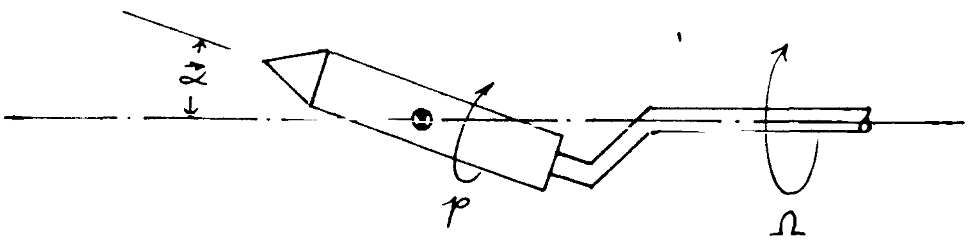

* An air bearing may be adaptable to this type installation.

If the model and sting are statically balanced about the sting axis of rotation, then only aerodynamic or externally applied moments can cause sting rotation.

With both driving and damping moments in the Magnus plane, the coning motion becomes analogus to the rolling motion of a canted-fin missile, i. e., there will be an initial acceleration, $\dot{\Omega}$, proportional to the driving moment and a steady-state Ω dependent upon both the driving and damping moments. From time histories of Ω obtained at various values of the axial spin rate and angle of attack, it should be possible to determine at least the aerodynamic coefficients $N_{p\alpha}$, $N_{p\alpha^3}$, N_{α^3}, N_{λ}, $N_{\lambda\alpha^2}$, and N_{λ^3} through the use of curve fitting techniques.

The aerodynamic driving moments can be provided in several ways. At large angles of attack, the asymmetric vortex separation will provide the driving moment. Magnus-type moments can also be generated by large axial spin, or in the case of a finned body, by the spin-rate generated by fin cant. Another means of driving a finned model, is by having the fins locked-in to a roll orientation which produces a side moment. Auxiliary drive systems, such as air jets, can be used to drive the model to an initially large Ω, and then data can also be obtained during the decay of Ω. The latter method will permit the damping moments to be measured under conditions where the aerodynamic driving moments are small, thus assisting in the separation of the driving and damping coefficients for a particular model.

The above technique has two advantages over the use of models with three degrees-of-rotational-freedom. First, there are no inertial moments introduced, as in the case where the magnitude of the angle of attack can change. Secondly, if the model has complete rotational freedom, all of the aerodynamic moments have to be evaluated, whereas with the above approach we do not have to isolate the pitching moment or pitch-yaw coupling terms.

Experiments for Vertical Wind Tunnel

It is believed that a vertical wind tunnel, such as the NASA Langley facility, offers advantages for studying the dynamics of large angle of attack near-circular motions of axi-symmetric body-fin configurations. Particularly, if quasi-steady circular motions can be obtained in the vertical tunnel, these should be describable by analytical solutions such as those derived in Sections II and V of the present report. Also, these motions could be correlated with predictions based on experimental data obtained with less degrees-of-freedom.

Another area where the vertical tunnel can be used advantageously is in the study of the initiation of non-planar or near-circular motions. Although in some cases circular limit cycles can be initiated by dynamic instability at small angles of attack, it is believed that most configurations will require moderate angle of attack, and possibly an initial coning motion, before a sustained non-planar or near-circular motion can be developed. One means of imparting these initial conditions is by the use of a body-fixed trim in conjunction with axial spin to produce a near resonant motion.* As the model approaches resonance,** the rolling trim will not only increase, but will be close to a pure lunar motion. If the motion grows into a circular limit cycle, it will become steadily less dependent upon the trim moment and at the angle of attack corresponding to the circular limit cycle the trim moment will probably be small as compared with the total overturning moment.

---

* It is believed that this mechanism is responsible for initiating large angle of attack post-resonance coning motions in canted-fin sounding rockets as well as in other types of finned bodies such as bombs.

** A variation in spin rate can be achieved by using canted fins, and launching the model at a spin rate much less than the steady-state spin rate.

The transient motion leading up to a sustained circular motion can be investigated at great length, as many parameters are involved. Although at present the vertical tunnel is limited to low subsonic velocities, an understanding of the dynamics in this regime should be a prelude to investigations at transonic and supersonic conditions.

VIII. CONCLUSIONS

The polar equations of yawing motion, which utilize the total angle of attack and the rotation of the angle of attack plane as the dependent variables, can be used to provide a better understanding of near-circular and non-planar motions than is possible with the conventional aeroballistic equations which express the angle of attack in complex variables. With the polar equations, nonlinear damping moments, various Magnus effects, and other aerodynamic nonlinearities (both conforming and not conforming to the Maple-Synge symmetry relationships) can be expanded into coefficients related to the angle of attack and Magnus planes. The simultaneous effect of both these terms and the nonlinear inertial moments, on the amplitude, frequency, and stability of circular limit motions can easily be ascertained by pertubation analysis.

An important result of the present analyses is that circular limit cycles are possible for all axi-symmetric missiles which possess a Magnus moment of sufficient magnitude, even though all the aerodynamic coefficients including the Magnus moment coefficient are linear. In addition, there exist a number of aerodynamic mechanisms for producing psuedo Magnus moments, which will also lead to non-planar and near-circular motions.

The present effort provides a suitable background for the design of non-planar motion experiments in wind tunnels and the extension of the cross-flow theory to include the effects of angle of attack plane rotation.

Appendix A. EFFECT OF MIRROR SYMMETRY ON CUBIC COEFFICIENTS

To show the effect of mirror symmetry, we can assume a set of right hand body-fixed axes as depicted in the sketch below, and consider the effect of the transformation associated with a reversal of the z axis. If the body possesses minor symmetry it should not be possible to distinguish between the coefficients for the two sets of axes.

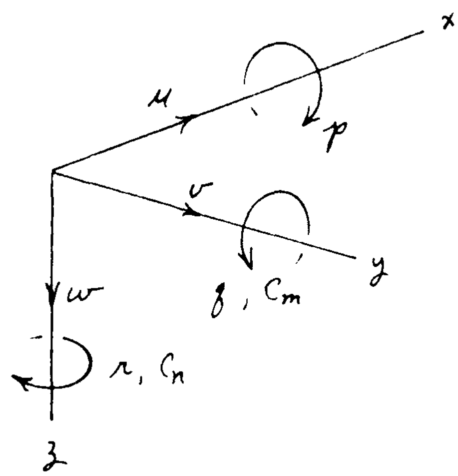

In affecting the transformed quantities, it will be noted that the positive quantities are those which correspond to a particular operation on the coordinate system. For example, in the basic coordinates p rotates y to z, q rotates z to x, and r rotates x to y. These rotations and their corresponding torques are defined as positive.

Using these definitions we have for the transformed axes the following positive quantities:

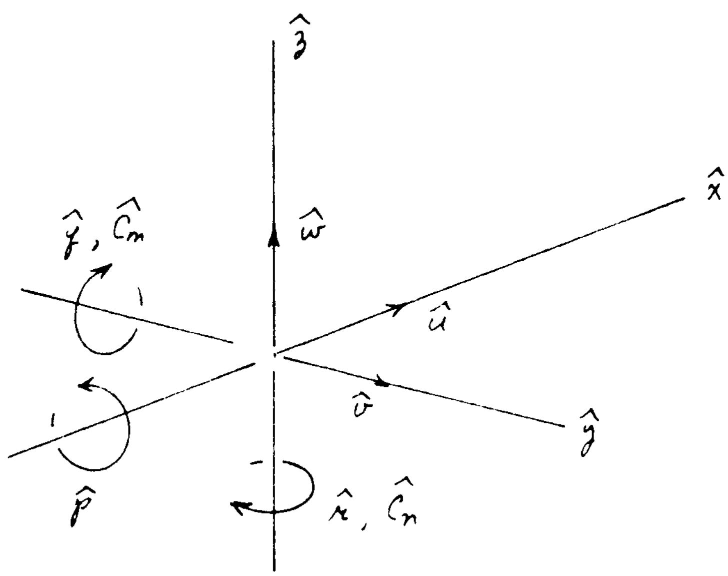

Comparison of the original and transformed axes show that

$$\hat{p} = -p$$
$$\hat{v} = v$$
$$\hat{w} = -w$$
$$\hat{r} = r$$
$$\hat{q} = -q$$
$$\hat{C}_m = -C_m$$
$$\hat{C}_n = C_n$$
$$\hat{\xi} = \hat{v} + i\hat{w} = v - iw = \bar{\xi}$$
$$\hat{\mu} = \hat{q} + i\hat{r} = -q + ir = -\bar{\mu}$$
$$\hat{\xi}' = \bar{\xi}'$$
$$\hat{\mu}' = -\bar{\mu}'$$

Let us now consider the effect of mirror symmetry on a specific cubic coefficient, as an example.

The Maple-Synge theory states that there should be imaginary coefficients in the moment expansion vanishing if r + s is odd, where r and s are related to the Maple-Synge power series expansion $(\mu)^{r}$, $(\bar{\mu})^{s}$, $(\omega)^{r}$, $(\bar{\omega})^{s}$.

A typical r + s odd term is Murphy's $D_{100}\, \xi \bar{\xi} \xi'$,* where the D_{100} coefficient may be complex and which we shall first assume to be expressed in terms of the Maple-Synge variables as

$$d_{100_{REAL}}(\mu, \bar{\mu}, \omega) + i\, d_{100_{IMAG.}}(\mu, \bar{\mu}, \omega)$$

Since $\mu \bar{\mu} = \mu_1^2 + \mu_2^2 = \delta^2$, a real number, and $\omega = \omega_1 + i\omega_2$, we have that

$$\xi \bar{\xi} \xi' = \mu \bar{\mu} \omega = \delta^2(\omega_1 + i\omega_2)$$

The moment expansion is now

$$C_m + i C_n = d_{100_{REAL}}\left[\delta^2\omega_1 + i\delta^2\omega_2\right] + d_{100_{IMAG.}}\left[i\delta^2\omega_1 - \delta^2\omega_2\right]$$

For the transformed axes we have

$$\begin{aligned}
\hat{C}_m + i\hat{C}_n &= -C_m + iC_n \\
&= d_{100_{REAL}}\left[-\delta^2\omega_1 + i\delta^2\omega_2\right] + d_{100_{IMAG}}\left[i\delta^2\omega_1 + \delta^2\omega_2\right] \\
&= d_{100_{REAL}}\left[\delta^2\hat{\omega}_1 + i\delta^2\hat{\omega}_2\right] + d_{100_{IMAG}}\left[-i\delta^2\hat{\omega}_1 + \delta^2\hat{\omega}_2\right]
\end{aligned}$$

from which it can be seen that $d_{100_{IMAG}}$ must vanish, in accordance with the Maple-Synge statement.

---

* This is a term defined by Murphy in Ref. 9.

Let us now assume the variables $\xi \; \bar{\xi} \; \xi' \; \bar{\xi}'$ to be equivalent to the Maple-Synge variables $\mu, \bar{\mu}, \omega, \bar{\omega}$. This is the usual aeroballistic approach, where the derivative of the angle of attack is taken to represent the cross angular velocity, viz. $\xi' = i\mu$

Now consider the term

$$d_{100_{REAL}}(\xi, \bar{\xi}, \xi') + i\, d_{100_{IMAG.}}(\xi, \bar{\xi}, \xi')$$

We have that

$$C_m + iC_n = d_{100_{REAL}}(v^2 + w^2)(v' + iw') + i\, d_{100_{IMAG}}(v^2 + w^2)(v' + iw')$$

and as above we obtain

$$\hat{C}_m + i\hat{C}_n = -d_{100_{REAL}}(\hat{v}^2 + \hat{w}^2)(\hat{v}' + i\hat{w}') + i\, d_{100_{IMAG}}(\hat{v}^2 + \hat{w}^2)(\hat{v}' + i\hat{w}')$$

In this case it is clear that $d_{100_{REAL}}$ must vanish, which is in contrast to the result obtained with the Maple-Synge variables. Thus, the choice of variables is very important when the effects of mirror symmetry are considered. The basic difficulty is that different transformations are obtained for rotation and translation vectors. Thus, different transformations are obtained for $\xi = \frac{v + iw}{V}$ and $\xi = \beta + i\alpha$, when the derivatives of ξ are considered.

PARAMETER	ASSUMED VALUES			
	STABLE $C_{m_\alpha} < 0$		UNSTABLE $C_{m_\alpha} > 0$	
	SMALL $C_{n_{p\alpha}}$	LARGE $C_{n_{p\alpha}}$	SMALL $C_{n_{p\alpha}}$	LARGE $C_{n_{p\alpha}}$
C_{m_α}	-12.7	-12.7	3.18	3.18
$C_{n_{p\alpha}}$	± 9.55	± 95.5	± 2.4	± 24.0
$C_{n_{\sigma\dot{\lambda}}}$	-212	-212	-26.5	-26.5
I_x / I	0.05	0.05	0.1	0.1
I'	10^4	10^4	10^4	10^4

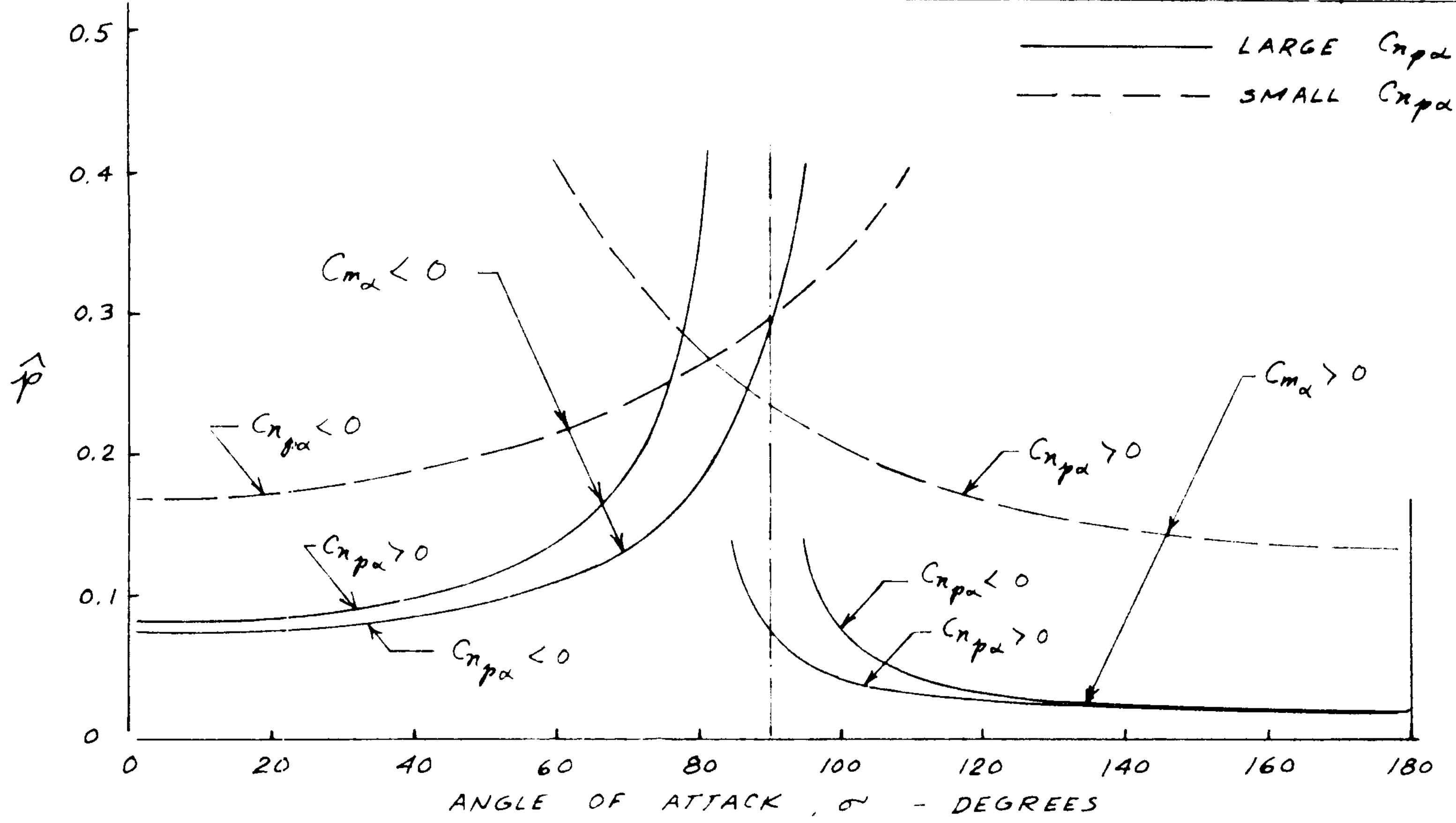

Fig. 1. Circular Motion Solutions

LIST OF REFERENCES

1. Brunk, James E., "The Dynamics and Aerodynamics of Self-Sustained Large Angle of Attack Body Spinning Motions," AFOSR-4596, February 1963.

2. Klinar, Walter J. and William D. Grantham, "Investigation of the Stability of Very Flat Spins and Analysis of Effects of Applying Various Moments Utilizing the Three Moment Equations of Motion," NASA Memo Report 5-25-59L, June 1959.

3. Murphy, Charles H., "Free-Flight Motion of Symmetric Missiles," BRL Report No. 1216, July 1963.

4. Zaroodny, Serge J. and Earl E. Bomberger, "Spiral Yawing Motions of 81mm M56 Shell - A Study in Non-Linear Theory," BRL Report No. 682, May 1953.

5. Haseltine, William R., "Notes on Murphy's Method," NOTS TP 3251, April 1963.

6. Murphy, Charles H., "Prediction of the Motion of Missiles Acted on by Non-Linear Forces and Moments," BRL Report No. 995, October 1956.

7. Murphy, Charles H., "The Measurement of Non-Linear Forces and Moments by Means of Free Flight Tests,", BRL Report No. 974, February 1956.

8. Maple, C. G. and J. L. Synge, "Aerodynamic Symmetry of Projectiles," Q. A. M., January 1949, Vol. VI, pp 345-366.

9. Murphy, Charles H., "Limit Cycles for Non-Spinning Statically Stable Symmetric Missiles," BRL Report No. 1071, March 1959.

10. Zaroodny, S. J., "Exercises on Maple-Synge Analysis of Consequences of Symmetry," BRL Report No. 930, February 1955.

11. Allen, H. Julian, "Estimation of the Forces and Moments Acting on Inclined Bodies of Revolution of High Fineness Ratio," NACA RM A9126, November 14, 1949.

12. Kelley, Howard R., "The Estimation of Normal Force and Pitching Moment Coefficients for Blunt-Based Bodies of Revolution at Large Angles of Attack," NOTS TM-998, May 27, 1953.

13. Allen, H. Julian and Edward W. Perkins, "Characteristics of Flow Over Inclined Bodies of Revolution," NACA RM A50L07, March 5, 1951.

14. Bursnall, William J. and Laurence K. Loftin, Jr., "Experimental Investigation of the Pressure Distribution About a Yawed Circuit Cylinder in the Critical Reynolds Number Range," NACA TN 2463, September 1961.

15. Perkins, Edward W. and Donald M. Kuehn, "Comparison of the Experimental and Theoretical Distributions of Lift on a Slender Inclined Body of Revolution at M = 2," NACA TN 3715, May 1956.

16. Dunn, Eldon L., "A Low-Speed Experimental Study of Yaw Forces on Bodies of Revolution at Large Angles of Pitch and Zero Angle of Sideslip," NOTS TM-1588, March 8, 1954.

17. Letko, William, "A Low-Speed Experimental Study of the Directional Characteristics of a Sharp-Nosed Fuselage Through a Large Angle-of-Attack Range at Zero Angle of Sideslip," NACA TN 2911, March 1953.

18. Curry, Warren H. and James F. Reed, "Measurement of Magnus Effects on a Sounding Rocket Model in a Supersonic Wind Tunnel," AIAA Paper No. 66-754, September 21-23, 1966.

19. Thompson, K. D., and D. F. Morrison, "The Asymmetric Shedding of Vortices from Slender Cylindrical Bodies at Large Angles of Yaw," Australian Weapons Research Establishment Technical Note HSA 106, May 1965.

20. Kelly, Howard R., "An Analytical Method for Predicting the Magnus Forces and Moments on Spinning Projectiles," NOTS TM-1634, August 12, 1954.

21. Krahn, E., "Negative Magnus Force," Journal of Aeronautical Sciences, Vol. 23, No. 4, p 377, April 1956.

22. Platou, Anders S., "Magnus Characteristics of Finned and Nonfinned Projectiles," AIAA Journal, Vol. 3, No. 1, January 1965.

23. Tobak, Murray and William R. Wehrend, "Stability Derivatives of Cones at Supersonic Speeds," NACA TN 3788, September 1956.

24. Ohman, L. H., " A Surface Flow Solution and Stability Derivatives for Bodies of Revolution in Complex Supersonic Flow — Part 1 - Theory and Some Representative Results," National Research Council of Canada, Aeronautical Report LR-418, November 1964.

25. Fink, Martin R., " Hypersonic Dynamic Stability of Sharp and Blunt Slender Cones," United Aircraft Corp. Research Laboratories Report, NASA Ascension No. X65-13609, July 15, 1964.

26. Margolis, Kenneth, "Theoretical Evaluation of the Pressures, Forces, and Moments at Hypersonic Speeds Acting on Arbitrary Bodies of Revolution Undergoing Separate and Combined Angle-of-Attack and Pitching Motions, "NASA TN D-652, June 1961

27. Tobak, Murray and Henry C. Lessing, "Study of the Aerodynamic Forces and Moments on Bodies of Revolution in Combined Pitching and Yawing Motions," NASA TN D-316, May 1960.

28. Brunk, James E., "Aerobee 150A Roll Lock-In Study," Alpha Research Inc., Report No. 65-9566-7, November 1965.

29. Loptien, G. W., "An Investigation of Cone-Cylinder Bodies in the Steady State Spin Mode and Magnus Force Effects on a Cone-Cylinder Body," WADD TN 60-76, August 1960.

30. Bird, John D. and Jacob H. Lichtenstein, "Wind-Tunnel Experiments Concerning the Dynamic Behavior of a Low-Speed Slowly Spinning Fin-Stabilized Rocket," NACA RM L54D22, July 6, 1954.

31. Lichtenstein, Jacob H., and James L. Williams, "A Wind-Tunnel Investigation of the Stability of the Antisubmarine Rocket MK 1 MOD O," NACA RM SL52K05, November 13, 1952.

32. Rodman, Ray, "Non-Linear Aerodynamic Normal Force and Moment on Slender Blunt - Based Bodies of Revolution with Laminar Boundary Layer," October 2,1966, (no report number).

NOMENCLATURE

C_{L_α} = lift coefficient derivative

C_D = drag coefficient

C_N = Normal force coefficient

C_{M_α} = aeroballistic moment coefficient

$C_{M_q} = \dfrac{\partial C_m}{\partial \frac{qd}{V}}$, aeroballistic pitch damping coefficient

$C_{M_{\dot\alpha}} = \dfrac{\partial C_m}{\partial \frac{\dot\alpha d}{V}}$, aeroballistic angle of attack damping coefficient

$C_{M_{p\alpha}} = \dfrac{\partial C_n}{\partial \frac{pd}{V} \partial \alpha}$, aeroballistic Magnus moment coefficient

$C_m = \dfrac{M}{\frac{1}{2}\rho V^2 S d}$, aerodynamic moment coefficient

$C_n = \dfrac{N}{\frac{1}{2}\rho V^2 S d}$, aerodynamic moment coefficient

d = aerodynamic reference length

G = Maple-Synge moment

g = Maple-Synge moment coefficient

H = Murphy aerodynamic damping parameter,

$$\frac{\rho s d}{2m}\left[\gamma C_{L_\alpha} - C_D - k_r^{-2}\left(C_{M_q} + \gamma C_{M_{\dot\alpha}}\right)\right]$$

I_x = axial moment of inertia

I = transverse moment of inertia

$i = \sqrt{-1}$

k, K = arbitrary constant or parameter

$k_t = \sqrt{I/md^2}$

$k_a = \sqrt{I_x/md^2}$

m = mass

M = overturning moment, angle of attack plane

N = moment in Magnus plane

M = Murphy moment parameter,

$$\frac{\rho S d}{2m}\left[\gamma k_t^{-2} C_{M_\alpha} - \gamma C_{L_\alpha}' \right]$$

n = number of fins

p, q, r = angular velocity of missile

$P = \frac{pd}{V} \frac{I_x}{I}$

S = aerodynamic reference area

T = Murphy aerodynamic Magnus moment parameter,

$$\frac{\rho S d}{2m}\left[\gamma C_{L_\alpha} + k_a^{-2} C_{M_{p\alpha}} \right]$$

$u = u_1, u_2, u_3$ (Maple-Synge velocity components)

u, v, w = components of velocity

V = total velocity

x, y, z = body axes

x, y', z' = fixed-plane axes

X, Y, Z = inertial reference axes

ρ = air density

γ = $\cos \vec{\alpha}$

$\vec{\alpha}$ = total angle of attack

ϵ = deflection of velocity vector

ω = total angular velocity of missile

ω = $\omega_1, \omega_2, \omega_3$, Maple-Synge angular velocity components

Ω = angular velocity of moving coordinate system

ξ = $\frac{v + i w}{V}$, complex angle of attack

δ = $|\xi|$

μ = complex angular velocity

θ = argument of complex variable

θ, ψ, ϕ = Euler angles

λ, σ = Euler angles

$\hat{\nu}$ = $\frac{\Omega, d}{V}$

Δ = differential quantity

$(\ )'$ = derivative with respect to non-dimensional length,

$\dot{(\ )}$ = derivative with respect to time

$\overline{(\ )}$ = conjugate of complex variable

$\widehat{(\ )}$ = transformed quantity